

Particle Physics from Stars

Georg G. Raffelt

Max-Planck-Institut für Physik (Werner-Heisenberg-Institut)
Föhringer Ring 6, 80805 München, Germany

KEYWORDS: astroparticle physics, stellar evolution, neutrinos, axions

ABSTRACT: Low-mass particles such as neutrinos, axions, other Nambu-Goldstone bosons and gravitons are produced in the hot and dense interior of stars. Therefore, astrophysical arguments constrain the properties of these particles in ways which are often complementary to cosmological arguments and to laboratory experiments. This review provides an update on the most important stellar-evolution limits and discusses them in the context of other information from cosmology and laboratory experiments.

24 March 1999

Prepared for the
Annual Review of Nuclear and Particle Science
Vol. 49 (1999)

CONTENTS

INTRODUCTION	3
THE SUN	4
<i>Basic Energy-Loss Argument</i>	4
<i>Solar Neutrino Measurements</i>	5
<i>Helioseismology</i>	6
<i>“Strongly” Interacting Particles</i>	6
LIMITS ON STELLAR ENERGY LOSSES	7
<i>Globular-Cluster Stars</i>	7
<i>White Dwarfs</i>	11
<i>Old Neutron Stars</i>	13
SUPERNOVAE	13
<i>SN 1987A Neutrino Observations</i>	13
<i>Signal Dispersion</i>	14
<i>Energy-Loss Argument</i>	15
<i>Radiative Neutrino Decays</i>	16
<i>Explosion Energetics</i>	17
<i>Neutrino Spectra and Neutrino Oscillations</i>	18
LIMITS ON NEUTRINO PROPERTIES	19
<i>Masses and Mixing</i>	19
<i>Dipole and Transition Moments</i>	20
<i>Millicharged Particles</i>	24
<i>Nonstandard Weak Interactions</i>	25
AXIONS AND OTHER PSEUDOSCALARS	26
<i>Interaction Structure</i>	26
<i>Limits on the Interaction Strength</i>	28
<i>Cosmological Limits</i>	32
LONG-RANGE FORCES	33
<i>Fifth Force</i>	33
<i>Leptonic and Baryonic Gauge Interactions</i>	34
<i>Time-Variation of Newton’s Constant</i>	34
<i>Equivalence Principle</i>	35
<i>Photon Mass</i>	36
<i>Multibody Neutrino Exchange</i>	37
CONCLUSION	37

1 INTRODUCTION

Astrophysical and cosmological arguments and observations have become part of the main-stream methodology to obtain empirical information on existing or hypothetical elementary particles and their interactions. The “heavenly laboratories” are complementary to accelerator and non-accelerator experiments, notably at the “low-energy frontier” of particle physics, which includes the physics of neutrinos and other weakly interacting low-mass particles such as the hypothetical axions, novel long-range forces, and so forth.

The present review is dedicated to stars as particle-physics laboratories, or more precisely, to what can be learned about weakly interacting low-mass particles from the observed properties of stars. The prime argument is that a hot and dense stellar plasma emits low-mass weakly interacting particles in great abundance. They subsequently escape from the stellar interior directly, without further interactions, and thus provide a local energy sink for the stellar medium. The astronomically observable impact of this phenomenon provides some of the most powerful limits on the properties of neutrinos, axions, and the like.

Once the particles have escaped they can decay on their long way to Earth, allowing one to derive interesting limits on radiative decay channels from the absence of unexpected x- or γ -ray fluxes from the Sun or other stars.

Finally, the weakly interacting particles can be directly detected at Earth, thus far only the neutrinos from the Sun and supernova (SN) 1987A, allowing one to extract important information on their properties.

The material covered here has been reviewed in 1990, with a focus on axion limits, by Turner [1] and by Raffelt [2], and a very brief “Mini-Review” was included in the 1998 edition of the Review of Particle Physics [3]. My 1996 book *Stars as Laboratories for Fundamental Physics* [4] treats these topics in much greater detail than is possible here. The present chapter is intended as a compact, up-to-date, and easily accessible source for the most important results and methods.

The subject of “Particle Physics from Stars” is broader than both my expertise and the space available here. I will not touch on the solar neutrino problem and its oscillation interpretation—this is a topic unto itself and has been extensively reviewed by other authors, for example [5, 6, 7].

The high densities encountered in neutron stars make them ideal for studies and speculations concerning novel phases of nuclear matter (e.g. meson condensates or quark matter), an area covered by two recent books [8, 9]. Quark stars are also the subject of an older review [10] and are covered in the proceedings of two topical conferences [11, 12].

Certain grand unified theories predict the existence of primordial magnetic monopoles. They would get trapped in stars and then catalyze the decay of nucleons by the Rubakov-Callan effect. The ensuing anomalous energy release is constrained by the properties of stars, in particular neutron stars and white dwarfs, a topic that has been reviewed a long time ago [13]. It was re-examined, and the limits improved, in the wake of the discovery of the faintest white dwarf ever detected which puts restrictive limits on an anomalous internal heat source [14].

Weakly interacting massive particles (WIMPs), notably in the guise of the supersymmetric neutralinos, are prime candidates for the cosmic dark matter. Some of them would get trapped in stars, annihilate with each other, and produce

a secondary flux of high-energy neutrinos. The search for such fluxes from the Sun and the center of the Earth by present-day and future neutrino telescopes is the “indirect method” to detect galactic particle dark matter, an approach which is competitive with direct laboratory searches—see [15] for a review.

Returning to the topics which are covered here, Sections 2–4 are devoted to a discussion of the main stellar objects that have been used to constrain low-mass particles, viz. the Sun, globular-cluster stars, compact stars, and SN 1987A. In Sections 5–7 the main constraints on neutrinos, axions, and novel long-range forces are summarized. Section 8 is given over to brief concluding remarks.

2 THE SUN

2.1 Basic Energy-Loss Argument

The Sun is the best-known star and thus a natural starting point for our survey of astrophysical particle laboratories. It is powered by hydrogen burning which amounts to the net reaction $4p + 2e^- \rightarrow {}^4\text{He} + 2\nu_e + 26.73 \text{ MeV}$, giving rise to a measured ν_e flux which now provides one of the most convincing indications for neutrino oscillations [5, 6, 7]. Instead of neutrinos from nuclear processes we focus here on particle fluxes which are produced in thermal plasma reactions. The photo neutrino process $\gamma + e^- \rightarrow e^- + \nu\bar{\nu}$ is a case in point, as is the production of gravitons from electron bremsstrahlung. The solar energy loss from such standard processes is small, but it may be large for new particles. To be specific we consider axions (Sec. 6) which arise in a variety of reactions, and in particular by the Primakoff process in which thermal photons mutate into axions in the electric field of the medium’s charged particles (Fig. 1). In Sec. 6.2.1 we will discuss direct search experiments for solar axions, while here we focus on what is the main topic of this review, the backreaction of a new energy loss on stars.



Figure 1: Primakoff production of axions in the Sun.

The Sun is a normal star which supports itself against gravity by thermal pressure, as opposed to degenerate stars like white dwarfs which are supported by electron degeneracy pressure. If one pictures the Sun as a self-gravitating monatomic gas in hydrostatic equilibrium, the “atoms” obey the virial theorem $\langle E_{\text{kin}} \rangle = -\frac{1}{2} \langle E_{\text{grav}} \rangle$. The most important consequence of this relationship is that extracting energy from such a system, i.e. reducing the total energy $\langle E_{\text{kin}} \rangle + \langle E_{\text{grav}} \rangle$, leads to contraction and to an *increase* of $\langle E_{\text{kin}} \rangle$. Therefore, all else being equal, axion losses lead to contraction and heating. The nuclear energy generation rate scales with a high power of the temperature. Therefore, the heating implied by the new energy loss causes increased nuclear burning—the star finds a new equilibrium configuration where the new losses are compensated by an increased rate of energy generation.

The main lesson is that the new energy loss does not “cool” the star; it leads to heating and an increased consumption of nuclear fuel. The Sun, where energy is

transported from the central nuclear furnace by radiation, actually overcompensates the losses and brightens, while it would dim if the energy transfer were by convection. Either behavior is understood by a powerful “homology argument” where the nonlinear interplay of the equations of stellar structure is represented in a simple analytic fashion [16].

The solar luminosity is well measured, yet this brightening effect is not observable because all else need not be equal. The present-day luminosity of the Sun depends on its unknown initial helium mass fraction Y ; in a solar model Y has to be adjusted such that $L_{\odot} = 3.85 \times 10^{33} \text{ erg s}^{-1}$ is reproduced after 4.6×10^9 years of nuclear burning. For solar models with axion losses the required presolar helium abundance Y as a function of the axion-photon coupling constant $g_{a\gamma}$ is shown in Table 1. The axion luminosity L_a is also given as well as the central helium abundance Y_c , density ρ_c , and temperature T_c of the present-day Sun.

Even axion losses as large as L_{\odot} can be accommodated by reducing the presolar helium mass fraction from about 27% to something like 23% [17, 18]. The “standard Sun” has completed about half of its hydrogen-burning phase. Therefore, the anomalous energy losses cannot exceed approximately L_{\odot} or else the Sun could not have reached its observed age. Indeed, for $g_{10} = 30$ no consistent present-day Sun could be constructed for any value of Y [18]. The emission rate of other hypothetical particles would have a different temperature and density dependence than the Primakoff process, yet the general conclusion remains the same that a novel energy loss must not exceed approximately L_{\odot} .

2.2 Solar Neutrino Measurements

This crude limit is improved by the solar neutrino flux which has been measured in five different observatories with three different spectral response characteristics, i.e. by the absorption on chlorine, gallium, and by the water Cherenkov technique. The axionic solar models produce larger neutrino fluxes; in Table 1 we show the expected detection rates for the Cl, Ga, and H₂O experiments relative to the standard case. For $g_{10} \lesssim 10$ one can still find oscillation solutions to the observed ν_e deficit, but larger energy-loss rates appear to be excluded [17].

Once the neutrino oscillation hypothesis has been more firmly established and the mixing parameters are better known, the neutrino measurements may be used to pin down the central solar temperature, allowing one to constrain novel energy losses with greater precision. For now it appears safe to conclude that the Sun

Table 1: Solar-model parameters and relative detection rates in the Cl, Ga, and water neutrino observatories as a function of the axion-photon coupling constant $g_{10} \equiv g_{a\gamma}/(10^{-10} \text{ GeV}^{-1})$ according to Ref. [17].

g_{10}	L_a [L_{\odot}]	Y	Y_c	ρ_c [g cm ⁻³]	T_c [10 ⁷ K]	Cl	Ga	H ₂ O
0	0	0.266	0.633	153.8	1.563	1	1	1
4.5	0.04	0.265	0.641	158.0	1.575	1.07	1.16	1.20
10	0.20	0.257	0.679	177.5	1.626	1.45	2.2	2.4
15	0.53	0.245	0.751	218.3	1.722	2.5	6.0	6.7
20	1.21	0.228	0.914	324.2	1.931	6.4	20	23

does not emit more than a few tenths of L_\odot in new forms of radiation.

2.3 Helioseismology

Over the past few years the precision measurements of the solar p-mode frequencies have provided a more reliable way to study the solar interior. For example, the convective surface layer is found to reach down to $0.710\text{--}0.716 R_\odot$ [19], the helium content of these layers to exceed 0.238 [20]. Gravitational settling has reduced the surface helium abundance by about 0.03 so that the presolar value must have been at least 0.268, in good agreement with standard solar models. The reduced helium content required of the axionic solar models in Table 1 disagrees significantly with this lower limit for $g_{10} \geq 10$.

One may also invert the p-mode measurements to construct a “seismic model” of the solar sound-speed profile, e.g. [21]. All modern standard solar models agree well with the seismic model within its uncertainties (shaded band in Fig. 2) which mostly derive from the inversion method itself, not the measurements. The difference between the sound-speed profile of a standard solar model and those including axion losses are also shown in Fig. 2. For $g_{10} \geq 10$ the difference is larger than the uncertainties of the seismic model, implying a limit

$$g_{a\gamma} \lesssim 10 \times 10^{-10} \text{ GeV}^{-1}. \quad (1)$$

Other cases may be different in detail, but it appears safe to assume that any new energy-loss channel must not exceed something like 10% of L_\odot .

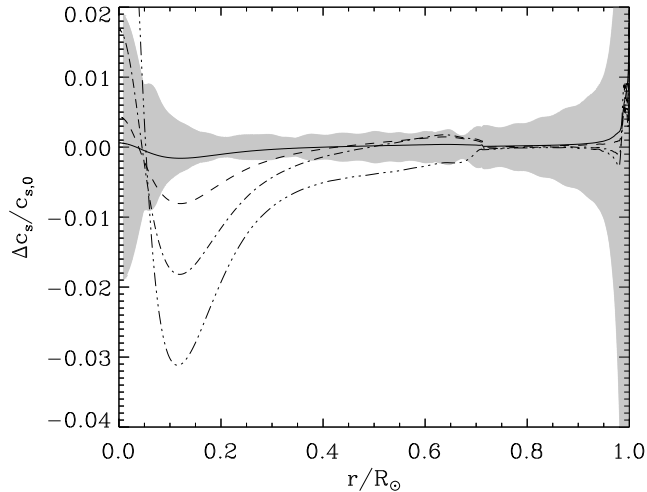


Figure 2: Fractional difference in sound-speed profiles of solar models with axion losses compared to the reference model [17]. The shaded area is the uncertainty of the seismic model [20]. The axion-photon coupling constant was $g_{10}=4.5$ (solid line), 10 (short-dashed), 15 (dash-dotted), 20 (dash-dot-dot-dotted).

2.4 “Strongly” Interacting Particles

Thus far we have assumed that the new particles couple so weakly that they escape from the stellar interior without further interactions, in analogy to neutrinos or gravitons. They emerge from the entire stellar volume, i.e. their emission

amounts to a local energy sink for the stellar plasma. But what if the particles interact so strongly that their mean free path is less than the solar radius?

The impact of such particles on a star compares to that of photons, which are also “trapped” by their “strong” interaction. Their continuous thermal production and re-absorption amounts to the net transfer of energy from regions of higher temperature to cooler ones. In the Sun this radiative form of energy transfer is more important than conduction by electrons or convection, except in the outer layers. A particle which interacts more weakly than photons is more effective because it travels a larger distance before re-absorption—the ability to transfer energy is proportional to the mean free path. The properties of the Sun roughly confirm the standard photon opacities, so that a new particle would have to interact more strongly than photons to be allowed [22, 23].

Therefore, contrary to what is sometimes stated in the literature, a new particle is by no means allowed just because its mean free path is less than the stellar dimensions. The impact of a new particle is maximal when its mean free path is of order the stellar radius. Of course, usually one is interested in very weakly interacting particles so that this point is moot.

3 LIMITS ON STELLAR ENERGY LOSSES

3.1 Globular-Cluster Stars

3.1.1 Evolution of Low-Mass Stars

The discussion in the previous section suggests that the emission of new weakly interacting particles from stars primarily modifies the time scale of evolution. For the Sun this effect is less useful to constrain particle emission than, say, the modified p-mode frequencies or the direct measurement of the neutrino fluxes. However, the observed properties of other stars provide far more restrictive limits on their evolutionary time scales so that anomalous modes of energy loss can be far more tightly constrained. We begin with globular-cluster stars which, together with SN 1987A, are the most successful example of astronomical observations that provide nontrivial limits on the properties of elementary particles.

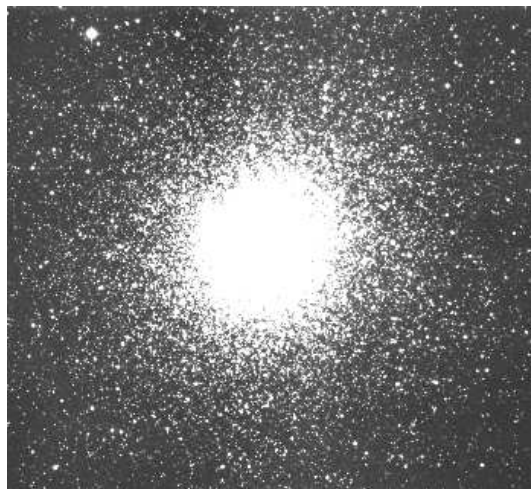


Figure 3: Globular cluster M3. (Image courtesy of Palomar/Caltech.)

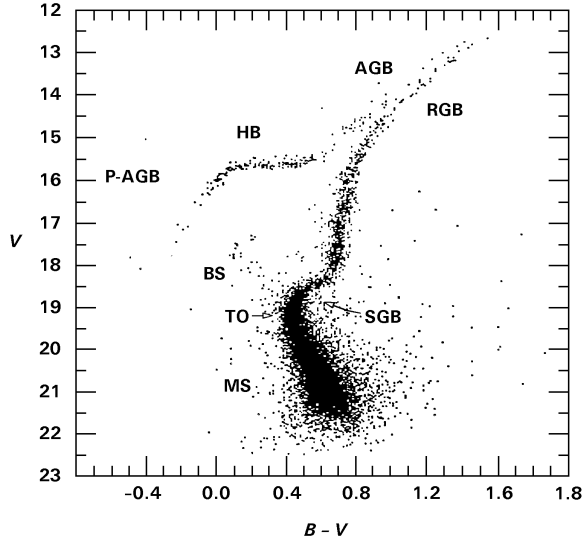


Figure 4: Color-magnitude diagram for the globular cluster M3, based on the photometric data of 10,637 stars [24]. Vertically is the brightness in the visual (V) band, horizontally the difference between B (blue) and V brightness, i.e. a measure of the color and thus surface temperature, where blue (hot) stars lie toward the left. The classification for the evolutionary phases is as follows [25]. MS (main sequence): core hydrogen burning. BS (blue stragglers). TO (main-sequence turnoff): central hydrogen is exhausted. SGB (subgiant branch): hydrogen burning in a thick shell. RGB (red-giant branch): hydrogen burning in a thin shell with a growing core until helium ignites. HB (horizontal branch): helium burning in the core and hydrogen burning in a shell. AGB (asymptotic giant branch): helium and hydrogen shell burning. P-AGB (post-asymptotic giant branch): final evolution from the AGB to the white-dwarf stage.

Our galaxy has about 150 globular clusters such as M3 (Fig. 3) which are gravitationally bound systems of up to a million stars. In Fig. 4 the stars of the cluster M3 are arranged according to their color or surface temperature (horizontal axis) and brightness (vertical axis) in the usual way, leading to a characteristic pattern which allows for rather precise tests of the theory of stellar evolution, and notably for quantitative measurements of certain evolutionary time scales. Globular clusters are the oldest objects in the galaxy and thus almost as old as the universe. The stars in a given cluster all formed at about the same time with essentially the same chemical composition, differing primarily in their mass. Because more massive stars evolve faster, present-day globular-cluster stars are somewhat below¹ $1 M_{\odot}$ so that we are concerned with low-mass stars ($\mathcal{M} \lesssim 2 M_{\odot}$). Textbook expositions of stellar structure and evolution are [26, 27].

Stars begin their life on the main sequence (MS) where they burn hydrogen in their center. Different locations on the MS in a color-magnitude diagram like Fig. 4 correspond to different masses, with more massive stars shining more

¹The letter \mathcal{M} denotes stellar masses with $1 M_{\odot} = 2 \times 10^{33}$ g the solar mass. The letter M is traditionally reserved for the absolute stellar brightness (in magnitudes or mag). The total or bolometric brightness is defined as $M_{\text{bol}} = 4.74 - 2.5 \log_{10}(L/L_{\odot})$, with the solar luminosity $L_{\odot} = 3.85 \times 10^{33}$ erg s⁻¹.

brightly. When central hydrogen is exhausted the star develops a degenerate helium core, with hydrogen burning in a shell. Curiously, the stellar envelope expands, leading to a large surface area and thus a low surface temperature (red color)—they become “red giants.” The luminosity is governed by the gravitational potential at the edge of the growing helium core so that these stars become ever brighter: they ascend the red-giant branch (RGB). The higher a star on the RGB, the more massive and compact its helium core.

The core grows until about $0.5 \mathcal{M}_\odot$ when it has become dense and hot enough to ignite helium. The ensuing core expansion reduces the gravitational potential at its edge and thus lowers the energy production rate in the hydrogen shell source, dimming these stars. Helium ignites at a fixed core mass, but the envelope mass differs due to varying rates of mass loss on the RGB, leading to different surface areas and thus surface temperatures. These stars thus occupy the horizontal branch (HB) in the color-magnitude diagram. In Fig. 4 the HB turns down on the left (blue color) where much of the luminosity falls outside the V filter; in terms of the total or “bolometric” brightness the HB is truly horizontal.

Finally, when helium is exhausted, a degenerate carbon-oxygen core develops, leading to a second ascent on what is called the asymptotic giant branch (AGB). These low-mass stars cannot ignite their carbon-oxygen core—they become white dwarfs after shedding most of their envelope.

The advanced evolutionary phases are fast compared with the MS duration which is about 10^{10} yr for stars somewhat below $1 \mathcal{M}_\odot$. For example, the ascent on the upper RGB and the HB phase each take around 10^8 yr. Therefore, the distributions of stars along the RGB and beyond can be taken as an “isochrone” for the evolution of a single star, i.e. a time-series of snapshots for the evolution of a single star with a fixed initial mass. Put another way, the number distribution of stars along the different branches are a direct measure for the duration of the advanced evolutionary phases. The distribution along the MS is different in that it measures the distribution of initial masses.

3.1.2 Core Mass at Helium Ignition

Anomalous energy losses modify this picture in measurable ways. We first consider an energy-loss mechanism which is more effective in the degenerate core of a red giant before helium ignition than on the HB so that the post-RGB evolution is standard. Since an RGB-star’s helium core is supported by degeneracy pressure there is no feedback between energy-loss and pressure: the core is actually *cooled*. Helium burning ($3^4\text{He} \rightarrow ^{12}\text{C}$) depends very sensitively on temperature and density so that the cooling delays the ignition of helium, leading to a larger core mass \mathcal{M}_c , with several observable consequences.

First, the brightness of a red giant depends on its core mass so that the RGB would extend to larger luminosities, causing an increased brightness difference $\Delta M_{\text{HB}}^{\text{tip}}$ between the HB and the RGB tip. Second, an increased \mathcal{M}_c implies an increased helium-burning core on the HB. For a certain range of colors these stars are pulsationally unstable and are then called RR Lyrae stars. From the measured RR Lyrae luminosity and pulsation period one can infer \mathcal{M}_c on the basis of their so-called mass-to-light ratio A . Third, the increased \mathcal{M}_c increases the luminosity of RR Lyrae stars so that absolute determinations of their brightness M_{RR} allow one to constrain the range of possible core masses. Fourth, the number ratio R of HB stars vs. RGB stars brighter than the HB is modified.

These observables also depend on the measured cluster metallicity as well as the unknown helium content which is usually expressed in terms of Y_{env} , the envelope helium mass fraction. Since globular clusters formed shortly after the big bang, their initial helium content must be close to the primordial value of 22–25%. Y_{env} should be close to this number because the initial mass fraction is somewhat depleted by gravitational settling, and somewhat increased by convective dredge-up of processed, helium-rich material from the inner parts of the star.

An estimate of \mathcal{M}_c from a global analysis of these observables except A was performed in [28] and re-analysed in [4], A was used in [29], and an independent analysis using all four observables in [30]. In Fig. 5 we show the allowed core mass excess $\delta\mathcal{M}_c$ and envelope helium mass fraction Y_{env} from the analyses [4, 30]; references to the original observations are found in these papers.

Figure 5 suggests that, within the given uncertainties, the different observations overlap at the standard core mass ($\delta\mathcal{M}_c = 0$) and at an envelope helium abundance of Y_{env} which is compatible with the primordial helium abundance. Of course, the error bands do not have a simple interpretation because they combine observational and estimated systematic errors, which involve some subjective judgement by the authors. The difference between the two panels of Fig. 5 gives one a sense of how sensitive the conclusions are to these more arbitrary aspects of the analysis. As a nominal limit it appears safe to adopt $|\delta\mathcal{M}_c| \lesssim 0.025$ or $|\delta\mathcal{M}_c|/\mathcal{M}_c \lesssim 5\%$; how much additional “safety-margin” one wishes to include is a somewhat arbitrary decision which is difficult to make objective in the sense of a statistical confidence level.

In [4] it was shown that this limit can be translated into an approximate limit on the average anomalous energy-loss rate ϵ_x of a helium plasma,

$$\epsilon_x \lesssim 10 \text{ erg g}^{-1} \text{ s}^{-1} \quad \text{at } T \approx 10^8 \text{ K}, \quad \rho \approx 2 \times 10^5 \text{ g cm}^{-3}. \quad (2)$$

The density represents the approximate average of a red-giant core before helium ignition; the value at its center is about 10^6 g cm^{-3} . The main standard-model

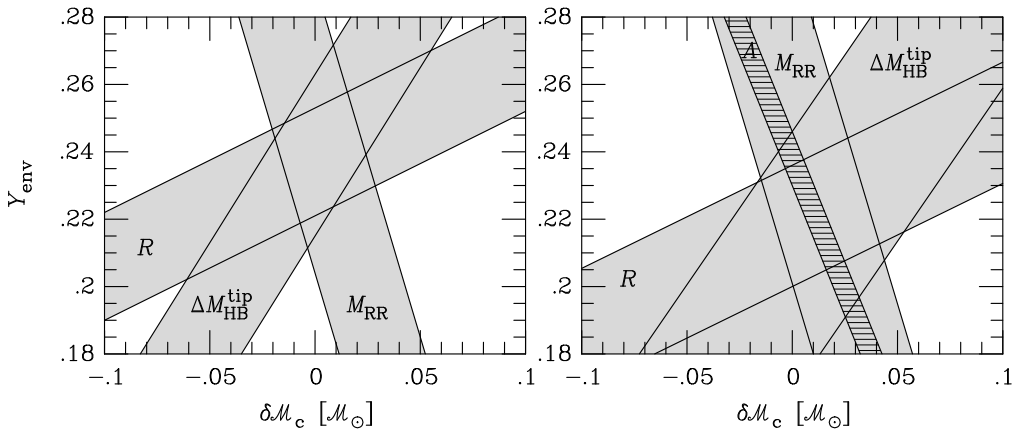


Figure 5: Allowed values for a core-mass excess at helium ignition $\delta\mathcal{M}_c$ and the envelope helium mass fraction Y_{env} of evolved globular-cluster stars. Left after [4], right after [30]. The observables are the brightness difference $\Delta M_{\text{HB}}^{\text{tip}}$ between the HB and the RGB tip, the RR Lyrae mass-to-light ratio A , their absolute brightness M_{RR} , and the number ratio R between HB and RGB stars.

neutrino emission process is plasmon decay $\gamma \rightarrow \nu\bar{\nu}$ with a core average of about $4 \text{ erg g}^{-1} \text{ s}^{-1}$. Therefore, Eq. (2) means that a new energy-loss channel must be less effective than a few times the standard neutrino losses.

3.1.3 Helium-Burning Lifetime of Horizontal-Branch Stars

We now turn to an energy-loss mechanism which becomes effective in a nondegenerate medium, i.e. we imagine that the core expansion after helium ignition “switches on” an energy-loss channel that was negligible on the RGB. Therefore, the pre-HB evolution is taken to be standard. As in the case of the Sun (Sec. 2.1) there will be little change in the HB stars’ brightness, rather they will consume their nuclear fuel faster and thus begin to ascend the AGB sooner. The net observable effect is a reduction of the number of HB relative to RGB stars.

From the measured HB/RGB number ratios in 15 globular clusters [31] and with plausible assumptions about the uncertainties of other parameters one concludes that the duration of helium burning agrees with stellar-evolution theory to within about 10% [4]. This implies that the new energy loss of the helium core should not exceed about 10% of its standard energy production rate. Therefore, the new energy-loss rate at average core conditions is constrained by [4]

$$\epsilon_x \lesssim 10 \text{ erg g}^{-1} \text{ s}^{-1} \quad \text{at} \quad T \approx 0.7 \times 10^8 \text{ K}, \quad \rho \approx 0.6 \times 10^4 \text{ g cm}^{-3}. \quad (3)$$

This limit is slightly more restrictive than the often-quoted “red-giant bound,” corresponding to $\epsilon_x \lesssim 100 \text{ erg g}^{-1} \text{ s}^{-1}$ at $T = 10^8 \text{ K}$ and $\rho = 10^4 \text{ g cm}^{-3}$. It was based on the helium-burning lifetime of the “clump giants” in open clusters [32]. They have fewer stars, leading to statistically less significant limits. The “clump giants” are the physical equivalent of HB stars, except that they occupy a common location at the base of the RGB, the “red-giant clump.”

3.1.4 Applications

After the energy-loss argument has been condensed into the simple criteria of Eqs. (2) and (3) it can be applied almost mechanically to a variety of cases. The main task is to identify the dominant emission process for the new particles and to calculate the energy-loss rate ϵ_x for a helium plasma at the conditions specified in Eqs. (2) or (3). The most important limits will be discussed in the context of specific particle-physics hypotheses in Secs. 5–7. Here we just mention that these and similar arguments were used to constrain neutrino electromagnetic properties [28, 29, 32, 33, 34, 35, 36, 37], axions [18, 38, 39, 40, 41, 42, 43, 44, 45, 46, 47, 48, 49, 50, 51, 52], paraphotons [53], the photo production cross section on ${}^4\text{He}$ of new bosons [54, 55], the Yukawa couplings of new bosons to baryons or electrons [56, 57], and supersymmetric particles [58, 59, 60].

One may also calculate numerical evolution sequences including new energy losses [18, 29, 35, 37, 52, 61]. Comparing the results from such studies with what one finds from Eqs. (2) and (3) reveals that, in view of the overall theoretical and observational uncertainties, it is indeed enough to use these simple criteria [4].

3.2 White Dwarfs

White dwarfs are another case where astronomical observations provide useful limits on new stellar energy losses. These compact objects are the remnants of

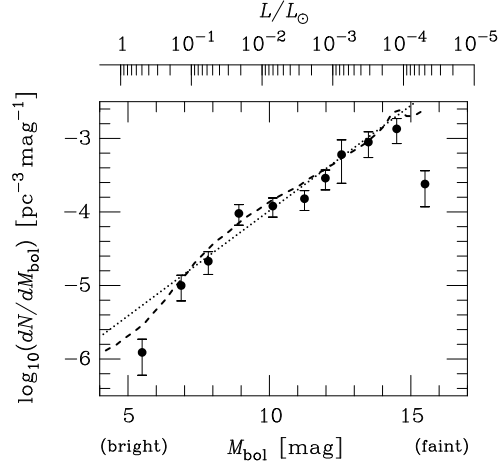


Figure 6: Observed white-dwarf luminosity function [63, 64]. The dotted line represents Mestel’s cooling law with a constant birthrate of $10^{-3} \text{ pc}^{-3} \text{ Gyr}^{-1}$. The dashed line is from the cooling curve of a $0.6 \mathcal{M}_{\odot}$ white dwarf which includes neutrino losses [65], assuming the same constant birthrate.

stars with initial masses of up to several \mathcal{M}_{\odot} [27, 62]. For low-mass progenitors the evolution proceeds as described in Sec. 3.1.1. When they ascend the asymptotic giant branch they eventually shed most of their envelope mass. The degenerate carbon-oxygen core, having reached something like $0.6 \mathcal{M}_{\odot}$, never ignites. Its subsequent evolution is simply one of cooling, first dominated by neutrino losses throughout its volume, later by surface photon emission.

The cooling speed can be observationally inferred from the “luminosity function,” i.e. the white-dwarf number density per brightness interval. As white dwarfs are intrinsically dim they are observed only in the solar neighborhood, out to perhaps 100 pc (1 pc = 3.26 ly) which is far less than the thickness of the galactic disk. The measured luminosity function (Fig. 6) reveals that there are few bright white dwarfs and many faint ones. The dotted line represents Mestel’s cooling law [62, 66], an analytic treatment based on surface photon cooling. The observed luminosity function dips at the bright end, a behavior ascribed to neutrino emission which quickly “switches off” as the star cools.

The luminosity function drops sharply at the faint end. Even the oldest white dwarfs have not yet cooled any further, implying that they were born 8–12 Gyr ago, in good agreement with the estimated age of the galaxy. Therefore, a novel cooling agent cannot be much more effective than the surface photon emission. This conclusion also follows from the agreement between the implied birthrate with independent estimates. The shape of the luminosity function can be deformed for an appropriate temperature dependence of the particle emission rate, e.g. enhancing the “neutrino dip” at the bright end. Finally, white dwarfs in a certain range of surface temperatures are pulsationally unstable and are then called ZZ Ceti stars. The pulsation period of a few minutes depends on the luminosity, the period decrease thus on the cooling speed. For G117–B15A the period change was measured [67, 68], implying a somewhat large cooling rate. While this discrepancy may be worrisome, probably these measurements should be taken as an approximate confirmation of the predicted white-dwarf cooling speed.

White dwarfs were used to constrain the axion-electron coupling [69, 70, 71, 72, 73, 74]. It was also noted that the somewhat large period decrease of G117–B15A could be ascribed to axion cooling [75]. Finally, a limit on the neutrino magnetic dipole moment was derived [73]. A detailed review of these limits is provided in [4]; they are somewhat weaker than those from globular-cluster stars, but on the same general level. Therefore, white-dwarf cooling essentially corroborates some of the globular-cluster limits, but does not improve on them.

3.3 Old Neutron Stars

Neutron stars are the compact remnants of stars with initial masses beyond about $8\mathcal{M}_\odot$. After their formation in a core-collapse supernova (Sec. 4) they evolve by cooling, a process that speeds up by a new energy-loss channel. Neutron-star cooling can now be observed by satellite-borne x-ray measurements of the thermal surface emission of several old pulsars—a recent review is [76].

Limits on axions were derived in [77, 78, 79], on neutrino magnetic dipole moments in [80]. These bounds are much weaker than those from SN 1987A or globular clusters. Turning this around, anomalous cooling effects by particle emission is probably not important in old neutron stars, leaving them as laboratories for many of the other uncertain bits of input physics such as the existence of new phases of nuclear matter [8, 9, 76, 81, 82]. If a neutron star converts into a strange-matter star an axion burst emerges [83], but for now this effect has not provided new empirical information on axion properties.

4 SUPERNOVAE

4.1 SN 1987A Neutrino Observations

When the explosion of the star Sanduleak –69 202 was detected on 23 February 1987 in the Large Magellanic Cloud, a satellite galaxy of our Milky Way at a distance of about 50 kpc (165,000 lyr), it became possible for the first time to measure the neutrino emission from a nascent neutron star, turning this supernova (SN 1987A) into one of the most important stellar particle-physics laboratories [84, 85, 86].

A type II supernova explosion [87, 88, 89, 90, 91, 92] is physically the implosion of an evolved massive star ($\mathcal{M} \gtrsim 8\mathcal{M}_\odot$) which has become an “onion-skin structure” with several burning shells surrounding a degenerate iron core. It cannot gain further energy by fusion so that it becomes unstable when it has reached the limiting mass (Chandrasekhar mass) of $1\text{--}2\mathcal{M}_\odot$ that can be supported by electron degeneracy pressure. The ensuing collapse is intercepted when the equation of state stiffens at around nuclear density ($3 \times 10^{14} \text{ g cm}^{-3}$), corresponding to a core size of a few tens of kilometers. At temperatures of tens of MeV this compact object is opaque to neutrinos. The gravitational binding energy of the newborn neutron star (“proto neutron star”) of about $3 \times 10^{53} \text{ erg}$ is thus radiated over several seconds from the “neutrino sphere.” Crudely put, the collapsed SN core cools by thermal neutrino emission from its surface.

The neutrino signal from SN 1987A (Fig. 7) was observed by the $\bar{\nu}_e p \rightarrow n e^+$ reaction in several detectors [86]. The number of events, their energies, and the distribution over several seconds corresponds well to theoretical expectations and thus has been taken as a confirmation of the standard picture that a compact

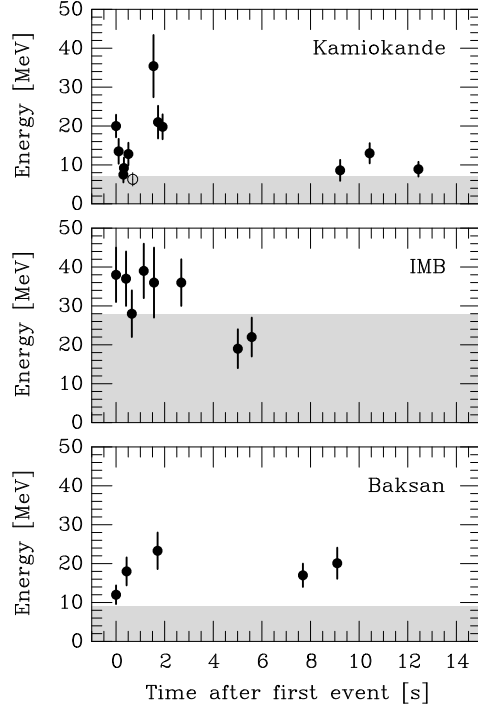


Figure 7: SN 1987A neutrino observations at Kamiokande [93], IMB [94] and Baksan [95]. The energies refer to the secondary positrons from the reaction $\bar{\nu}_e p \rightarrow n e^+$. In the shaded area the trigger efficiency is less than 30%. The clocks have unknown relative offsets; in each case the first event was shifted to $t = 0$. In Kamiokande, the event marked as an open circle is attributed to background.

remnant formed which emitted its energy by quasi-thermal neutrino emission. Detailed statistical analyses of the data were performed in [96, 97].

The signal does show a number of “anomalies.” The average $\bar{\nu}_e$ energies inferred from the Irvine-Michigan-Brookhaven (IMB) and Kamiokande observations are quite different [98, 99]. The large time gap of 7.3 s between the first 8 and the last 3 Kamiokande events looks worrisome [100]. The distribution of the final-state positrons from the $\bar{\nu}_e p \rightarrow n e^+$ capture reaction should be isotropic, but is found to be significantly peaked away from the direction of the SN [55, 101, 102]. In the absence of other explanations, these features have been blamed on statistical fluctuations in the sparse data.

4.2 Signal Dispersion

A dispersion of the neutrino burst can be caused by a time-of-flight delay from a nonvanishing neutrino mass [103]. The arrival time from SN 1987A at a distance D would be delayed by

$$\Delta t = 2.57 \text{ s} \left(\frac{D}{50 \text{ kpc}} \right) \left(\frac{10 \text{ MeV}}{E_\nu} \right)^2 \left(\frac{m_\nu}{10 \text{ eV}} \right)^2. \quad (4)$$

As the $\bar{\nu}_e$ were registered within a few seconds and had energies in the 10 MeV range, m_{ν_e} is limited to less than around 10 eV. Detailed analyses reveal that

the pulse duration is consistently explained by the intrinsic SN cooling time and that $m_{\nu_e} \lesssim 20$ eV is implied as something like a 95% CL limit [96, 104].

The apparent absence of a time-of-flight dispersion effect of the $\bar{\nu}_e$ burst was also used to constrain a “millicharge” of these particles (they would be deflected in the galactic magnetic field) [5, 105], a quantum field theory with a fundamental length scale [106], and deviations from the Lorentzian rule of adding velocities [107]. Limits on new long-range forces acting on the neutrinos [108, 109, 110, 111, 112] seem to be invalidated in the most interesting case of a long-range leptonic force by screening from the cosmic background neutrinos [113].

The SN 1987A observations confirm that the visual SN explosion occurs several hours after the core-collapse and thus after the neutrino burst. Again, there is no apparent time-of-flight delay of the relative arrival times between the neutrino burst and the onset of the optical light curve, allowing one to confirm the equality of the relativistic limiting velocity for these particle types to within 2×10^{-9} [114, 115]. Moreover, the Shapiro time delay in the gravitational field of the galaxy of neutrinos agrees with that of photons to within about 4×10^{-3} [116], constraining certain alternative theories of gravity [117, 118].

4.3 Energy-Loss Argument

The late events in Kamiokande and IMB reveal that the signal duration was not anomalously short. Very weakly interacting particles would freely stream from the inner core, removing energy which otherwise would power the late-time neutrino signal. Therefore, its observed duration can be taken as evidence against such novel cooling effects. This argument has been advanced to constrain axion-nucleon couplings [119, 120, 121, 122, 123, 124, 125, 126, 127], majorons [128, 129, 130, 131, 132, 133, 134], supersymmetric particles [135, 136, 137, 138, 139, 140, 141, 142], and graviton emission in quantum-gravity theories with higher dimensions [143, 144]. It has also been used to constrain right-handed neutrinos interacting by a Dirac mass term [120, 145, 146, 147, 148, 149, 150, 151, 152, 153, 154, 155], mixed with active neutrinos [156, 157], interacting through right-handed currents [120, 158, 159, 160, 161], a magnetic dipole moment [162, 163, 164, 165, 166], or an electric form factor [167, 168]. Many of these results will be reviewed in Secs. 5–7 in the context of specific particle-physics hypotheses.

Here we illustrate the general argument with axions (Sec. 6) which are produced by nucleon bremsstrahlung $NN \rightarrow NN a$ so that the energy-loss rate depends on the axion-nucleon Yukawa coupling g_{aN} . In Fig. 8 we show the expected neutrino-signal duration as a function of g_{aN} . With increasing g_{aN} , corresponding to an increasing energy-loss rate, the signal duration drops sharply. For a sufficiently large g_{aN} , however, axions no longer escape freely; they are trapped and thermally emitted from the “axion sphere” at unit optical depth. Beyond some coupling strength axions are less important than neutrinos and cannot be excluded.

However, particles which are on the “strong interaction” side of this argument need not be allowed. They could be important for the energy-transfer during the infall phase and they could produce events in the neutrino detectors. For example, “strongly coupled” axions in a large range of g_{aN} are actually excluded because they would have produced too many events by their absorption on ^{16}O [169].

Likewise, particles on the free-streaming side can cause excess events in the

neutrino detectors. For example, right-handed neutrinos escaping from the inner core could become “visible” by decaying into left-handed states [170] or by spin-precessing in the galactic magnetic field if they have a dipole moment.

Returning to the general argument, one can estimate a limit on the energy-loss rate on the free-streaming side by the simple criterion that the new channel should be less effective than the standard neutrino losses, corresponding to [4]

$$\epsilon_x \lesssim 10^{19} \text{ erg g}^{-1} \text{ s}^{-1} \quad \text{at} \quad \rho = 3 \times 10^{14} \text{ g cm}^{-3}, \quad T = 30 \text{ MeV}. \quad (5)$$

The density is the core average, the temperature an average during the first few seconds. Some authors find higher temperatures, but for a conservative limit it is preferable to stick to a value at the lower end of the plausible range. At these conditions the nucleons are partially degenerate while the electrons are highly degenerate. Several detailed numerical studies reveal that this simple criterion corresponds to approximately halving the neutrino signal duration [4].

A simple analytic treatment is far more difficult on the trapping side; see [121] for an example in the context of axions.

The SN 1987A energy-loss argument tends to be most powerful at constraining new particle interactions with nucleons. Therefore, it is necessary to calculate the interaction rate with a hot and dense nuclear medium that is dominated by many-body effects. Besides the sparse data, the theoretical treatment of the emission rate is the most problematic aspect of this entire method.

4.4 Radiative Neutrino Decays

If neutrinos have masses one expects that the heavier ones are unstable and decay radiatively as $\nu \rightarrow \nu' \gamma$. SN 1987A is thought to have emitted similar fluxes of neutrinos and antineutrinos of all flavors so that one would have expected a burst of γ -rays in coincidence with the neutrinos. No excess counts were observed in the gamma-ray spectrometer (GRS) on the solar maximum mission (SMM) satellite [171, 172], leading to restrictive limits on neutrino decays [171, 172, 173, 174, 175]. The GRS happened to go into calibration mode about 223 s after the neutrino burst, but for low-mass neutrinos ($m_\nu \lesssim 40 \text{ eV}$) the entire γ -ray burst would

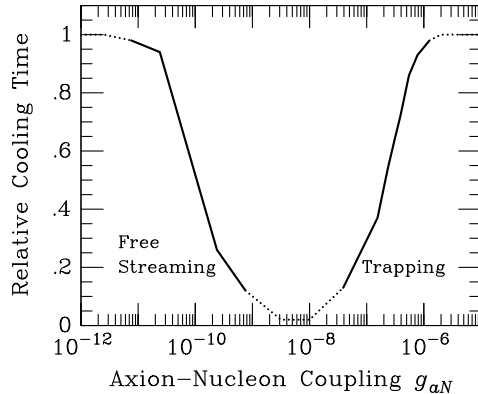


Figure 8: Relative duration of SN neutrino cooling as a function of the axion-nucleon coupling. Freely streaming axions are emitted from the entire core volume, trapped ones from the “axion sphere.” The solid line follows from the numerical calculations [124, 125]; the dotted line is an arbitrary continuation.

have been captured, leading to a radiative decay limit of [4]

$$\tau_\gamma/m_\nu \gtrsim 0.8 \times 10^{15} \text{ s/eV}. \quad (6)$$

For higher-mass neutrinos the photon burst would have been stretched beyond the GRS window. The first γ -rays from decays near the SN would arrive in coincidence with the $\bar{\nu}_e$ burst, but the γ -burst duration would be given by something like Eq. (4). As a further complication, such higher-mass neutrinos violate the cosmological mass limit unless they decay sufficiently fast and thus nonradiatively. Put another way, one must simultaneously worry about radiative and nonradiative decay channels—a detailed discussion is in [4].

Comparable limits in the higher-mass range were also derived from γ -ray data of the Pioneer Venus Orbiter (PVO) [176]. For $m_\nu \gtrsim 0.1$ MeV, decay photons still arrive years after SN 1987A. In 1991 the COMPTEL instrument aboard the Compton Gamma Ray Observatory looked at the SN 1987A remnant for about 0.68×10^6 s, providing the most restrictive limits in this mass range [177, 178].

For $m_\nu \gtrsim 2m_e \approx 1.2$ MeV, which is only possible for ν_τ with an experimental mass limit of about 18 MeV, the dominant radiative decay channel is $\nu_\tau \rightarrow \nu_e e^+ e^-$. From SN 1987A one would still expect γ -rays from the bremsstrahlung process $\nu_\tau \rightarrow \nu_e e^+ e^- \gamma$, leading to interesting limits [172, 176, 179, 180, 181].

The decay positrons from past galactic SNe would be trapped by the galactic magnetic fields and thus linger for up to 10^5 yr. Independently of SN 1987A, measurements of the galactic positron flux thus provide limits on neutrino decays with final-state positrons [4, 182].

4.5 Explosion Energetics

The standard scenario of a type II SN explosion has it that a shock wave forms near the edge of the core when its collapse halts at nuclear density and that this shock wave ejects the mantle of the progenitor star. However, in typical numerical calculations the shock wave stalls so that this “prompt explosion” scenario does not seem to work. In the “delayed explosion” picture the shock wave is revived by neutrino heating, perhaps in conjunction with convection, but even then it appears difficult to obtain a successful or sufficiently energetic explosion.

Therefore, one may speculate that nonstandard modes of energy transfer play an important role. An example is Dirac neutrinos with a magnetic dipole moment of order $10^{-12} \mu_B$ (Bohr magnetons). The right-handed (sterile) components would arise in the deep inner core by helicity-flipping collisions and escape. They precess back into interacting states in the large magnetic fields outside the SN core and heat the shock region; their interaction cross section would be relatively large because of their large inner-core energies [183, 184, 185, 186, 187, 188].

Certainly it is important not to deposit *too much* energy in the mantle and envelope of the star. 99% of the gravitational binding energy of the neutron star goes into neutrinos, about 1% into the kinetic energy of the explosion, and about 0.01% into the optical supernova. Therefore, neutrinos or other particles emitted from the core must not decay radiatively within the progenitor’s envelope radius of about 100 s or else too much energy lights up [189, 190].

4.6 Neutrino Spectra and Neutrino Oscillations

Neutrino oscillations can have several interesting ramifications in the context of SN physics because the temporal and spectral characteristics of the emission process depend on the neutrino flavor [90, 91, 92, 203]. The simplest case is that of the “prompt ν_e burst” which represents the deleptonization of the outer core layers at about 100 ms after bounce when the shock wave breaks through the edge of the collapsed iron core. This “deleptonization burst” propagates through the mantle and envelope of the progenitor star so that resonant oscillations take place for a large range of mixing parameters between ν_e and some other flavor, notably for most of those values where the MSW effect operates in the Sun [191, 192, 193, 194, 195, 196, 197, 198, 199, 200]. In a water Cherenkov detector this burst is visible as ν_e - e scattering, which is forward peaked, but one would have expected only a fraction of an event from SN 1987A. The first event in Kamiokande may be attributed to this signal, but this interpretation is statistically insignificant.

During the next few hundred milliseconds the shock wave stalls at a few hundred kilometers above the core and needs rejuvenating. The efficiency of neutrino heating can be increased by resonant flavor oscillations which swap the ν_e flux with, say, the ν_τ one. Therefore, what passes through the shock wave as a ν_e was born as a ν_τ at the proto neutron star surface. It has on average higher energies and thus is more effective at transferring energy. In Fig. 9 the shaded range of mixing parameters is where supernovae are helped to explode, assuming a “normal” neutrino mass spectrum with $m_{\nu_e} < m_{\nu_\tau}$ [201]. Below the shaded region the resonant oscillations take place beyond the shock wave and thus do not affect the explosion.

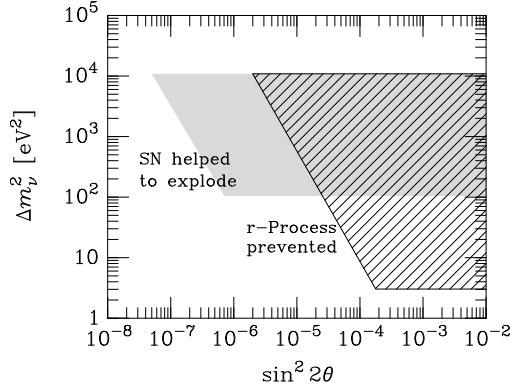


Figure 9: Mass difference and mixing between ν_e and ν_μ or ν_τ where a spectral swap would occur to help explode supernovae, schematically after [201], and where it would prevent r-process nucleosynthesis, schematically after [215, 216, 217].

The logic of this scenario depends on deviations from strictly thermal neutrino emission at some blackbody “neutrino sphere.” The neutrino cross sections are very energy dependent and different for different flavors so that the concept of a neutrino sphere is rather crude—the spectra are neither thermal nor equal for the different flavors [202, 203]. The dominant opacity source for ν_e is the process $\nu_e + n \rightarrow p + e^-$, for $\bar{\nu}_e$ it is $\bar{\nu}_e + p \rightarrow n + e^+$, while for $\nu_{\mu,\tau}$ and $\bar{\nu}_{\mu,\tau}$ it is neutral-current scattering on nucleons. Therefore, unit optical depth is at

the largest radius (and lowest medium temperature) for ν_e , and deepest (highest temperature) for $\nu_{\mu,\tau}$ and $\bar{\nu}_{\mu,\tau}$. In typical calculations one finds a hierarchy $\langle E_{\nu_e} \rangle : \langle E_{\bar{\nu}_e} \rangle : \langle E_{\text{others}} \rangle \approx \frac{2}{3} : 1 : \frac{5}{3}$ with $\langle E_{\bar{\nu}_e} \rangle = 14\text{--}17$ MeV [92]. The SN 1987A observations imply a somewhat lower range of $\langle E_{\bar{\nu}_e} \rangle \approx 7\text{--}14$ MeV [96, 99].

It should be noted that, pending a more detailed numerical confirmation [204], the difference between the $\bar{\nu}_e$ and $\nu_{\mu,\tau}$ or $\bar{\nu}_{\mu,\tau}$ average energies appears to be smaller than commonly assumed [126, 205, 206, 207], but there is no doubt that the ν_e spectrum is softer than the others. Still, the quantitative import of flavor oscillations depends on details of the neutrino spectra formation process in those SN core layers where the diffusion approximation for the neutrino transport is no longer valid, yet neutrinos are still trapped.

A few seconds after core bounce the shock wave has long since taken off, leaving behind a relatively dilute “hot bubble” above the neutron-star surface. This region is one suspected site for r-process heavy-element synthesis, which requires a neutron-rich environment [208, 209, 210, 211, 212, 213, 214]. The neutron-to-proton ratio, which is governed by the β reactions $\nu_e + n \rightarrow p + e^-$ and $\bar{\nu}_e + p \rightarrow n + e^+$, is shifted to a neutron-rich phase if $\langle E_{\nu_e} \rangle < \langle E_{\bar{\nu}_e} \rangle$ as for standard neutrino spectra. Resonant oscillations can again swap the ν_e flux with another one, inverting this hierarchy of energies. In the hatched range of mixing parameters shown in Fig. 9 the r-process would be disturbed [215, 216, 217, 218]. On the other hand, $\nu_e \rightarrow \nu_s$ oscillations into a sterile neutrino could actually help the r-process by removing some of the neutron-stealing ν_e [219, 236].

A large body of recent literature was devoted to explaining the large kick velocities of the observed radio pulsars as a “neutrino rocket effect.” The required few-percent anisotropy of the SN neutrino emission was attributed to an intricate interplay between the magnetic-field induced neutrino dispersion relation and resonant oscillations [220, 221, 222, 223, 224, 225, 226, 227]. However, due to a conceptual error the effect was vastly overestimated [228] so that the pulsar kicks do not seem to be related to neutrino oscillations in any obvious way.

If the mixing angle between ν_e and some other flavor is large, the $\bar{\nu}_e$ flux from a SN contains a significant fraction of oscillated states that were born as $\bar{\nu}_\mu$ or $\bar{\nu}_\tau$ and thus should have higher average energies. The measured SN 1987A event energies are already somewhat low, a problem so strongly exacerbated by oscillations that a large-mixing-angle solution of the solar neutrino deficit poses a problem [99, 104, 229]. This conclusion, however, depends on the standard predictions for the average neutrino energies which may not hold up to closer scrutiny as mentioned above.

5 LIMITS ON NEUTRINO PROPERTIES

5.1 Masses and Mixing

Astrophysics and cosmology play a fundamental role for neutrino physics as the properties of stars and the universe at large provide some of the most restrictive limits on nonstandard properties of these elusive particles. Therefore, it behoves us to summarize what the astrophysical arguments introduced in the previous sections teach us about neutrinos.

Unfortunately, stars do not tell us very much about neutrino masses, the holy grail of neutrino physics. The current discourse [230, 231, 232] centers on the interpretation of the solar [7] and atmospheric [233] neutrino anomalies and

the LSND experiment [234, 235] which all provide very suggestive evidence for neutrino oscillations. Solar neutrinos imply a Δm_ν^2 of about 10^{-5} eV² (MSW solutions) or 10^{-10} eV² (vacuum oscillations), atmospheric neutrinos 10^{-3} – 10^{-2} eV², and the LSND experiment 0.3–8 eV². Taken together, these results require a fourth flavor, a sterile neutrino, which is perhaps the most spectacular implication of these experiments, but of course also the least secure.

Core-collapse supernovae appear to be the only case in stellar astrophysics, apart from the solar neutrino flux, where neutrino oscillations can be important. However, Fig. 9 reveals that the experimentally favored mass differences negate a role of neutrino oscillations for the explosion mechanism or r-process nucleosynthesis, except perhaps when sterile neutrinos exist [219, 236]. Oscillations affect the interpretation of the SN 1987A signal [99, 104, 229] and that of a future galactic SN [237, 238, 239]. However, as discussed in Sec. 4.6, the main challenge is to develop a quantitatively more accurate understanding of supernovae as neutrino sources before relying on relatively fine points of the neutrino spectral characteristics to learn about neutrino mixing parameters.

Oscillation experiments reveal only mass *differences* so that one still needs to worry about the absolute neutrino mass scale. The absence of anomalous SN 1987A signal dispersion (Sec. 4.2) gives a limit [96, 104]

$$m_{\nu_e} \lesssim 20 \text{ eV}, \quad (7)$$

somewhat weaker than current laboratory bounds. A high-statistics observation of a galactic SN by a detector like Superkamiokande could improve this limit to about 3 eV by using the fast rise-time of the neutrino burst as a measure of dispersion effects [240]. If the neutrino mass differences are indeed very small, this limit carries over to the other flavors. One can derive an independent mass limit on ν_μ and ν_τ in the range of a few 10 eV if one identifies a neutral-current signature in a water Cherenkov detector [241, 242, 243, 244, 245], or if a future neutral-current detector provides an additional measurement [246, 247].

The SN 1987A energy-loss argument (Sec. 4.3) provides a limit on a neutrino Dirac mass of [4, 120, 145, 146, 147, 148, 152]

$$m_\nu(\text{Dirac}) \lesssim 30 \text{ keV}. \quad (8)$$

It is based on the idea that trapped Dirac neutrinos produce their sterile component with a probability of about $(m_\nu/2E_\nu)^2$ in collisions and thus feed energy into an invisible channel. This result was important in the discourse on Simpson's 17 keV neutrino which is now only of historical interest [248].

5.2 Dipole and Transition Moments

5.2.1 Electromagnetic Form Factors

Neutrino electromagnetic interactions would provide for a great variety of astrophysical implications. In the vacuum, the most general neutrino interaction with the electromagnetic field is [249, 250]

$$\mathcal{L}_{\text{int}} = -F_1 \bar{\psi} \gamma_\mu \psi A^\mu - G_1 \bar{\psi} \gamma_\mu \gamma_5 \psi \partial_\mu F^{\mu\nu} - \frac{1}{2} \bar{\psi} \sigma_{\mu\nu} (F_2 + G_2 \gamma_5) \psi F^{\mu\nu}, \quad (9)$$

where ψ is the neutrino field, A^μ the electromagnetic vector potential, and $F^{\mu\nu}$ the field-strength tensor. The form factors are functions of Q^2 with Q the energy-momentum transfer. In the $Q^2 \rightarrow 0$ limit F_1 is the electric charge, G_1 an anapole moment, F_2 a magnetic, and G_2 an electric dipole moment.

If neutrinos are electrically strictly neutral, corresponding to $F_1(0) = 0$, they still have a charge radius, usually defined as $\langle r^2 \rangle = 6\partial F_1(Q^2)/e\partial Q^2|_{Q^2=0}$. This form factor provides for a contact interaction, not for a long-range force, and as such modifies processes with Z^0 exchange [251, 252, 253, 254, 255]. As astrophysics provides no precision test for the effective strength of neutral-current interactions, this form factor is best probed in laboratory experiments [256]. Likewise, the anapole interaction vanishes in the $Q^2 \rightarrow 0$ limit and thus represents a modification to the standard neutral-current interaction, with no apparent astrophysical consequences.

The most interesting possibility are magnetic and electric dipole and transition moments. If the standard model is extended to include neutrino Dirac masses, the magnetic dipole moment is $\mu_\nu = 3.20 \times 10^{-19} \mu_B m_\nu/eV$ where $\mu_B = e/2m_e$ is the Bohr magneton [249, 250]. An electric dipole moment ϵ_ν violates CP, and both are forbidden for Majorana neutrinos. Including flavor mixing implies electric and magnetic transition moments for both Dirac and Majorana neutrinos, but they are even smaller due to GIM cancellation. These values are far too small to be of any experimental or astrophysical interest. Significant neutrino electromagnetic form factors require a more radical extension of the standard model, for example the existence of right-handed currents.

5.2.2 Plasmon Decay in Stars

Dipole or transition moments allow for several interesting processes (Fig. 10). For the purpose of deriving limits, the most important case is $\gamma \rightarrow \nu\bar{\nu}$ which is kinematically possible in a plasma because the photon acquires a dispersion relation which roughly amounts to an effective mass. Even without anomalous couplings, the plasmon decay proceeds because the charged particles of the medium induce an effective neutrino-photon interaction. Put another way, even standard neutrinos have nonvanishing electromagnetic form factors in a medium [257, 258]. The standard plasma process [259, 260, 261] dominates the neutrino production in white dwarfs or the cores of globular-cluster red giants.

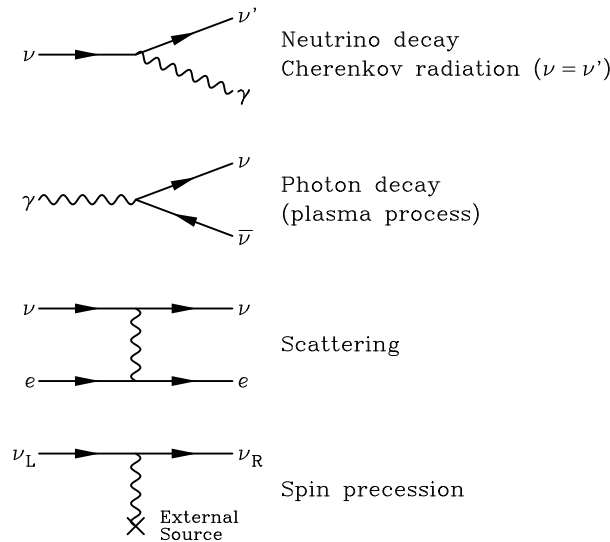


Figure 10: Processes with neutrino electromagnetic dipole or transition moments.

The plasma process was first used in [262] to constrain neutrino electromagnetic couplings. Numerical implementations of the nonstandard rates in stellar-evolution calculations are [29, 35, 37, 73]. The helium-ignition argument in globular clusters (Sec. 3.1.2), equivalent to Eq. (2), implies a limit [4, 28, 36, 37]

$$\mu_\nu \lesssim 3 \times 10^{-12} \mu_B, \quad (10)$$

applicable to magnetic and electric dipole and transition moments for Dirac and Majorana neutrinos. Of course, the final-state neutrinos must be lighter than the photon plasma mass which is around 10 keV for the relevant conditions.

The corresponding laboratory limits are much weaker [3]. The most restrictive bound is $\mu_{\nu_e} < 1.8 \times 10^{-10} \mu_B$ at 90% CL from a measurement of the $\bar{\nu}_e$ - e -scattering cross section involving reactor sources. A significant improvement should become possible with the MUNU experiment [263], but it is unlikely that the globular-cluster limit can be reached anytime soon.

5.2.3 Radiative Decay

A neutrino mass eigenstate ν_i may decay to another one ν_j by the emission of a photon, where the only contributing form factors are the magnetic and electric transition moments. The inverse radiative lifetime is found to be [249, 250]

$$\tau_\gamma^{-1} = \frac{|\mu_{ij}|^2 + |\epsilon_{ij}|^2}{8\pi} \left(\frac{m_i^2 - m_j^2}{m_i} \right)^3 = 5.308 \text{ s}^{-1} \left(\frac{\mu_{\text{eff}}}{\mu_B} \right)^2 \left(\frac{m_i^2 - m_j^2}{m_i^2} \right)^3 \left(\frac{m_i}{\text{eV}} \right)^3, \quad (11)$$

where μ_{ij} and ϵ_{ij} are the transition moments while $|\mu_{\text{eff}}|^2 \equiv |\mu_{ij}|^2 + |\epsilon_{ij}|^2$. Radiative neutrino decays have been constrained from the absence of decay photons of reactor $\bar{\nu}_e$ fluxes [264], the solar ν_e flux [265, 266], and the SN 1987A neutrino burst [171, 172, 173, 174, 175]. For $m_\nu \equiv m_i \gg m_j$ these limits can be expressed as

$$\frac{\mu_{\text{eff}}}{\mu_B} \lesssim \begin{cases} 0.9 \times 10^{-1} \text{ (eV}/m_\nu)^2 & \text{Reactor } (\bar{\nu}_e), \\ 0.5 \times 10^{-5} \text{ (eV}/m_\nu)^2 & \text{Sun } (\nu_e), \\ 1.5 \times 10^{-8} \text{ (eV}/m_\nu)^2 & \text{SN 1987A (all flavors),} \\ 1.0 \times 10^{-11} \text{ (eV}/m_\nu)^{9/4} & \text{Cosmic background (all flavors).} \end{cases} \quad (12)$$

In this form the SN 1987A limit applies for $m_\nu \lesssim 40$ eV as explained in Sec. 4.4. The decay of cosmic background neutrinos would contribute to the diffuse photon backgrounds, excluding the shaded areas in Fig. 11. They are approximately delineated by the dashed line, corresponding to the bottom line in Eq. (12). More restrictive limits obtain for certain masses above 3 eV from the absence of emission features from several galaxy clusters [270, 271, 387].

For low-mass neutrinos the m_ν^3 phase-space factor in Eq. (11) is so punishing that the globular-cluster limit is the most restrictive one for m_ν below a few eV. This is precisely the mass range which today appears favored from neutrino oscillation experiments. Turning this around, the globular-cluster limit implies that radiative decays of low-mass neutrinos do not seem to have observable consequences.

For masses above about 30 eV one must invoke fast invisible decays in order to avoid a conflict with the cosmological mass limit. In this case radiative decay limits involve the total lifetime as another parameter; the SN 1987A limits have been interpreted in this sense in [4, 174, 176, 178].

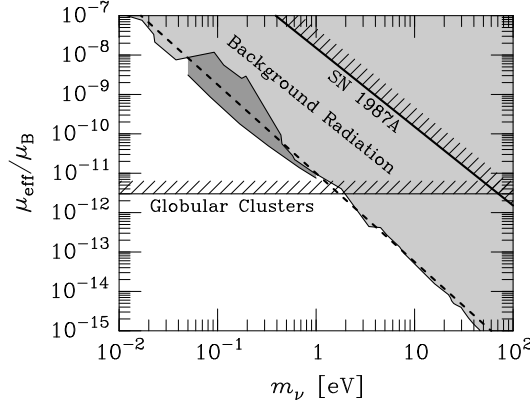


Figure 11: Astrophysical limits on neutrino dipole moments. The light-shaded background-radiation limits are from [267], the dark-shaded ones from [268, 269], the dashed line is the approximation formula in Eq. (12), bottom line.

5.2.4 Cherenkov Effect

Another form of “radiative decay” is the Cherenkov effect $\nu \rightarrow \nu + \gamma$, which involves the same initial- and final-state neutrino. This process is kinematically allowed for photons with $\omega^2 - \mathbf{k}^2 < 0$, which obtains in certain media or in external magnetic fields. The neutrino may have an anomalous dipole moment, but there is also a standard-model photon coupling induced by the medium or the external field. Thus far it does not look as if the neutrino Cherenkov effect has any strong astrophysical significance (see [272] for a review of the literature).

5.2.5 Spin-Flip Scattering

The magnetic or electric dipole interaction couples neutrino fields of opposite chirality. In the relativistic limit this implies that a neutrino flips its helicity in an “electromagnetic collision,” which in the Dirac case produces the sterile component. The active states are trapped in a SN core so that spin-flip collisions open an energy-loss channel in the form of sterile states. Conversely, the SN 1987A energy-loss argument (Sec. 4.3) allows one to derive a limit [163, 166],

$$\mu_\nu(\text{Dirac}) \lesssim 3 \times 10^{-12} \mu_B, \quad (13)$$

for both electric and magnetic dipole and transition moments. It is the same as the globular-cluster limit Eq. (10), which however includes the Majorana case.

Spin-flip collisions would also populate the sterile Dirac components in the early universe and thus increase the effective number of thermally excited neutrino degrees of freedom. Full thermal equilibrium is attained for $\mu_\nu(\text{Dirac}) \gtrsim 60 \times 10^{-12} \mu_B$ [34, 273]. In view of the SN 1987A and globular-cluster limits this result assures us that big-bang nucleosynthesis remains undisturbed.

5.2.6 Spin and Spin-Flavor Precession

Neutrinos with magnetic or electric dipole moments spin-precess in external magnetic fields [274, 275]. For example, solar neutrinos can precess into sterile and thus undetectable states in the Sun’s magnetic field [276, 277, 278]. The same

for SN neutrinos in the galactic magnetic field where an important effect obtains for $\mu_\nu \gtrsim 10^{-12} \mu_B$. Moreover, the high-energy sterile states emitted by spin-flip collisions from the inner SN core could precess back into active ones and cause events with anomalously high energies in SN neutrino detectors, an effect which probably requires $\mu_\nu(\text{Dirac}) \lesssim 10^{-12} \mu_B$ from the SN 1987A signal [163, 279]. For the same general μ_ν magnitude one may expect an anomalous rate of energy transfer to the shock wave in a SN, helping with the explosion (Sec. 4.5).

In a medium the refractive energy shift for active neutrinos relative to sterile ones creates a barrier to the spin precession [281, 282]. The mass difference has the same effect if the precession is between different flavors through a transition moment [280]. However, the mass and refractive terms may cancel, leading to resonant spin-flavor oscillations in the spirit of the MSW effect [283, 284, 285, 286]. This mechanism can explain all solar neutrino data [287, 288], but requires rather large toroidal magnetic fields in the Sun since the neutrino magnetic (transition) moments have to obey the globular-cluster limit of Eq. (10). For Majorana neutrinos, the spin-flavor precession amounts to transitions between neutrinos and antineutrinos so that the observation of antineutrinos from the Sun would be a diagnostic for this effect [289, 290, 291].

Large magnetic fields exist in SN cores so that spin-flavor precession could play an important role there, with possible consequences for the explosion mechanism, r-process nucleosynthesis, or the measurable neutrino signal [292, 293, 294, 295, 296]. The downside of this richness of phenomena is that there are so many unknown parameters (electromagnetic neutrino properties, masses, mixing angles) as well as the unknown magnetic field strength and distribution that it is difficult to come up with reliable limits or requirements on neutrino properties. The SN phenomenon is probably too complicated to serve as a laboratory to pin down electromagnetic neutrino properties, but it clearly is an environment where these properties could have far-reaching consequences.

5.3 Millicharged Particles

It is conceivable that neutrinos carry small electric charges if charge conservation is not exact [297, 298] or if the families are not sequential [299, 300, 301]. Moreover, new particles with small electric charges are motivated in certain models with a “mirror sector” and a slightly broken mirror symmetry [302]. Therefore, it is interesting to study the experimental, astrophysical, and cosmological bounds on “millicharged” particles [303, 304, 305, 306, 307].

A model-independent ν_e charge limit arises from the absence of dispersion of the SN 1987A neutrino signal in the galactic magnetic field [5, 105]

$$e_{\nu_e} \lesssim 3 \times 10^{-17} e. \quad (14)$$

If charge conservation holds in neutron decay, $e_{\nu_e} \lesssim 3 \times 10^{-21} e$ results, based on a limit for the neutron charge of $e_n = (-0.4 \pm 1.1) \times 10^{-21} e$ [308] and on the neutrality of matter which was found to be $e_p + e_e = (0.8 \pm 0.8) \times 10^{-21} e$ [309]. The measured ν_μ - e cross section implies $e_{\nu_\mu} \lesssim 10^{-9} e$ [305].

Generic millicharged particles (charge e_x , mass m_x) could appear as virtual states and would thus modify the Lamb shift unless $e_x < 0.11 e m_x / \text{MeV}$ [304]. A number of limits follow from a host of previous accelerator experiments [304] and a recent dedicated search at SLAC [310]—see Fig. 12.

Millicharged particles are produced by the plasmon decay process and thus drain energy from stars. In globular clusters, the emission rate is almost the same for HB stars and red giants before helium ignition, in contrast with the magnetic-dipole case. Therefore, Eqs. (2) and (3) give an almost identical limit [261]

$$e_x \lesssim 2 \times 10^{-14} e, \quad (15)$$

applicable for m_x below a few keV. The SN 1987A energy-loss argument extends the exclusion range to about 10 MeV for $10^{-9} e \lesssim e_x \lesssim 10^{-7} e$ [4, 167].

The usual big-bang nucleosynthesis (BBN) limit on the effective number of neutrino species N_{eff} provides another constraint. A millicharged neutrino is of Dirac nature so that its right-handed component adds one effective species. If the millicharged particles are not neutrinos, then depending on their spin N_{eff} may increase even more. If BBN excludes one extra species one finds $e_x \lesssim 3 \times 10^{-9} e$ for $m_x \lesssim 1$ MeV [304]. More stringent limits apply in certain models where the millicharged particles are associated with a shadow sector [307].

Further regions in Fig. 12 are excluded to avoid “overclosing” the universe by the new particles [304, 307]. However, because their relic density depends on their annihilation cross section, it is necessary to specify a model. It is hard to imagine new particles which interact solely through their small electric charge!

5.4 Nonstandard Weak Interactions

5.4.1 Right-Handed Currents

Right-handed (r.h.) weak interactions may exist on some level, e.g. in left-right symmetric models where the r.h. gauge bosons differ from the standard ones by their mass. In the low-energy limit relevant for stars one may account for the new couplings by a r.h. Fermi constant ϵG_F where ϵ is a small dimensionless parameter. In left-right symmetric models one finds explicitly for charged-current processes $\epsilon_{CC}^2 = \zeta^2 + [m(W_L)/m(W_R)]^2$ where $m(W_{L,R})$ are the l.h. and r.h. gauge boson masses and ζ is the left-right mixing parameter [158].

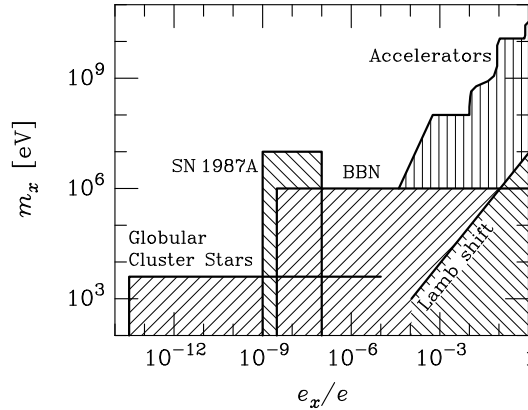


Figure 12: Limits on the electric charge e_x and mass m_x of generic millicharged particles which may be neutrinos or new particles. In order to avoid overclosing the universe, additional model-dependent parameter regions are excluded. The big-bang nucleosynthesis (BBN) excluded region is larger in some models.

Assuming that neutrinos are Dirac particles, a SN core loses energy into r.h. states as an “invisible channel” by the process $e + p \rightarrow n + \nu_{e,R}$. The SN 1987A energy-loss argument (Sec. 4.3) then requires $\epsilon_{CC} \lesssim 10^{-5}$ [4, 120, 158]. Laboratory experiments yield a weaker limit of order $\epsilon_{CC} \lesssim 3 \times 10^{-2}$ [311], but do not depend on the assumed existence of r.h. neutrinos.

For neutral currents the dominant emission process is $NN \rightarrow NN\nu_R\bar{\nu}_R$ which is subject to saturation effects as in the case of axion emission [126]. One then finds $\epsilon_{NC} \lesssim 3 \times 10^{-3}$ [4], somewhat less restrictive than the original limits of [120, 158]; see also [159, 160, 161]. This bound is also somewhat less restrictive than $\epsilon_{NC} \lesssim 10^{-3}$ found from big-bang nucleosynthesis [312].

5.4.2 Secret Neutrino Interactions and Majorons

The neutrino-neutrino cross section is not known experimentally. It could be anomalously large if neutrino Majorana masses were to arise from a suitable majoron model [313, 314, 315, 316]. “Secret” neutrino-neutrino interactions were constrained by the fact that the SN 1987A neutrino signal was not depleted by collisions with cosmic background neutrinos [317]. Supernova physics with majorons and SN 1987A limits were discussed in [128, 129, 130, 131, 132, 133, 134, 318, 319, 320, 321, 322, 323]. There is little doubt that majoron models will have an important impact on SN physics for neutrino-majoron Yukawa couplings in the 10^{-6} – 10^{-3} range. The existing literature, however, is too confusing for this author to come up with a clear synthesis of what SN physics implies for majoron models.

5.4.3 Flavor-Changing Neutral Currents

In certain models the neutrino neutral current has an effective flavor-changing component. Neutrinos propagating in matter then have medium-induced mixings and thus can oscillate even if they are strictly massless [324, 325]. Naturally, this phenomenon can be important for the oscillation of solar [326, 327, 328, 329] and supernova [330, 331] neutrinos.

6 AXIONS AND OTHER PSEUDOSCALARS

6.1 Interaction Structure

New spontaneously broken global symmetries imply the existence of Nambu-Goldstone bosons that are massless and as such present the most natural case (besides neutrinos) for using stars as particle-physics laboratories. Massless scalars would lead to new long-range forces (Sect. 7) so that we may focus here on pseudoscalars. The most prominent example are axions which were proposed more than twenty years ago as a solution to the strong CP problem [332, 333, 334, 335]; for reviews see [336, 337] and for the latest developments the proceedings of a topical conference [338]. We use axions as a generic example—it will be obvious how to extend the following results and discussions to other cases.

Actually, axions are only “pseudo Nambu-Goldstone bosons” in that the spontaneously broken chiral Peccei-Quinn symmetry $U_{PQ}(1)$ is also explicitly broken,

providing these particles with a small mass

$$m_a = 0.60 \text{ eV} \frac{10^7 \text{ GeV}}{f_a}. \quad (16)$$

Here, f_a is the Peccei-Quinn scale, an energy scale which is related to the vacuum expectation value of the field that breaks $U_{\text{PQ}}(1)$. The properties of Nambu-Goldstone bosons are always related to such a scale which is the main quantity to be constrained by astrophysical arguments, while Eq. (16) is specific to axions and allows one to express limits on f_a in terms of m_a .

In order to calculate the axionic energy-loss rate from stellar plasmas one needs to specify the interaction with the medium constituents. The interaction with a fermion j (mass m_j) is generically

$$\mathcal{L}_{\text{int}} = \frac{C_j}{2f_a} \bar{\Psi}_j \gamma^\mu \gamma_5 \Psi_j \partial_\mu a \quad \text{or} \quad -i \frac{C_j m_j}{f_a} \bar{\Psi}_j \gamma_5 \Psi_j a, \quad (17)$$

where Ψ_j is the fermion and a the axion field and C_j is a model-dependent coefficient of order unity. The combination $g_{aj} \equiv C_j m_j / f_a$ plays the role of a Yukawa coupling and $\alpha_{aj} \equiv g_{aj}^2 / 4\pi$ acts as an ‘‘axionic fine structure constant.’’ The derivative form of the interaction is more fundamental in that it is invariant under $a \rightarrow a + a_0$ and thus respects the Nambu-Goldstone nature of these particles. The pseudoscalar form is usually equivalent, but one has to be careful when calculating processes where two Nambu-Goldstone bosons are attached to one fermion line, for example an axion and a pion attached to a nucleon [120, 339, 340, 341, 342].

The dimensionless couplings C_i depend on the detailed implementation of the Peccei-Quinn mechanism. Limiting our discussion to ‘‘invisible axion models’’ where f_a is much larger than the scale of electroweak symmetry breaking, it is conventional to distinguish between models of the DFSZ type (Dine, Fischler, Srednicki [343], Zhitnitskiĭ [344]) and of the KSVZ type (Kim [345], Shifman, Vainshtein, Zakharov [346]). In KSVZ models, axions have no tree-level couplings to the standard quarks or leptons, yet axions couple to nucleons by their generic mixing with the neutral pion. The latest analysis gives numerically [127]

$$C_p = -0.34, \quad C_n = 0.01 \quad (18)$$

with a statistical uncertainty of about ± 0.04 and an estimated systematic uncertainty of roughly the same magnitude. The tree-level couplings to standard quarks and leptons in the DFSZ model depend on an angle β which measures the ratio of vacuum expectation values of two Higgs fields. One finds [127]

$$C_e = \frac{1}{3} \cos^2 \beta, \quad C_p = -0.07 - 0.46 \cos^2 \beta, \quad C_n = -0.15 + 0.38 \cos^2 \beta, \quad (19)$$

with similar uncertainties as in the KSVZ case.

The CP-conserving interaction between photons and pseudoscalars is commonly expressed in terms of an inverse energy scale $g_{a\gamma}$ according to

$$\mathcal{L}_{\text{int}} = \frac{1}{4} g_{a\gamma} F_{\mu\nu} \tilde{F}^{\mu\nu} a = -g_{a\gamma} \mathbf{E} \cdot \mathbf{B} a, \quad (20)$$

where F is the electromagnetic field-strength tensor and \tilde{F} its dual. For axions

$$g_{a\gamma} = \frac{\alpha}{2\pi f_a} C_\gamma, \quad C_\gamma = \frac{E}{N} - 1.92 \pm 0.08, \quad (21)$$

where E/N is the ratio of the electromagnetic and over color anomalies, a model-dependent ratio of small integers. In the DFSZ model or grand unified models one has $E/N = 8/3$, for which $C_\gamma \approx 0.75$, but one can also construct models with $E/N = 2$, which significantly reduces the axion-photon coupling [347]. The value of C_γ in a great variety of cases was reviewed in [348, 349].

6.2 Limits on the Interaction Strength

6.2.1 Photons

The axion interaction with fermions or photons allows for numerous reactions which can produce axions in stars, which may imply limits on the axion coupling strength. Beginning with photons, pseudoscalars interact according to the Lagrangian of Eq. (20) which allows for the decay $a \rightarrow 2\gamma$. In stellar plasmas the photon-axion interaction also makes possible the Primakoff conversion $\gamma \leftrightarrow a$ in the electric fields of electrons and nuclei [38]—see Fig. 1. For low-mass pseudoscalars the emission rate was calculated for various degrees of electron degeneracy in [48, 74, 350], superseding an earlier calculation where screening effects had been ignored [43].

The helioseismological constraint on solar energy losses then leads to Eq. (1) as a bound on $g_{a\gamma}$. Figure 13 shows this constraint (“Sun”) in the context of other bounds; similar plots are found in [3, 4, 351, 352, 353]. For axions the relationship between $g_{a\gamma}$ and m_a is indicated by the heavy solid line, assuming $E/N = 8/3$.

One may also search directly for solar axions. One method (“helioscope”) is to direct a dipole magnet toward the Sun, allowing solar axions to mutate into

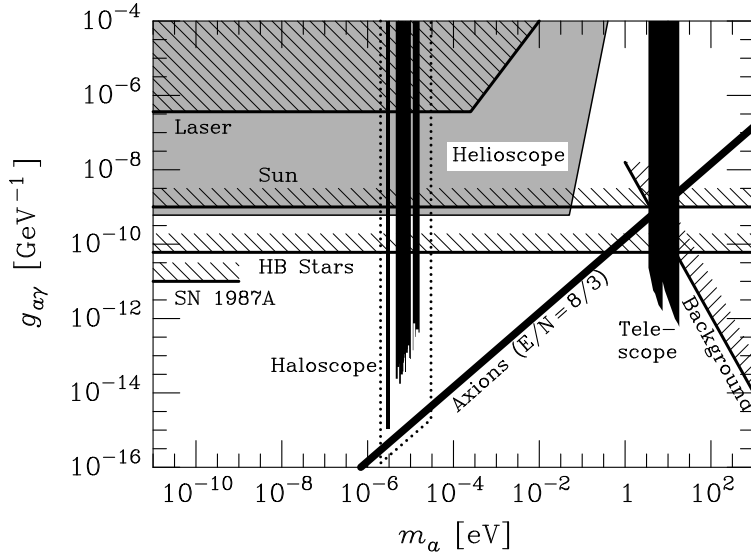


Figure 13: Limits to the axion-photon coupling $g_{a\gamma}$ as defined in Eq. (20). They apply to any pseudoscalar except for the “haloscope” search which assumes that these particles are the galactic dark matter; the dotted region marks the projected sensitivity range of the ongoing dark-matter axion searches. For higher masses than shown here the pertinent limits are reviewed in [352].

x-rays by the inverse Primakoff process [355, 356]. A pilot experiment was not sensitive enough [357], but the exposure time was significantly increased in a new experiment in Tokyo where a dipole magnet was gimballed like a telescope so that it could follow the Sun [358, 359]. The resulting limit $g_{a\gamma} \lesssim 6 \times 10^{-10} \text{ GeV}^{-1}$ is more restrictive than Eq. (1). Another helioscope project was begun in Novosibirsk several years ago [361], but its current status has not been reported for some time. An intriguing project (SATAN) at CERN would use a decommissioned LHC test magnet that could be mounted on a turning platform to achieve reasonable periods of alignment with the Sun [362]. This setup could begin to compete with the globular-cluster limit of Eq. (22).

The axion-photon transition in a macroscopic magnetic field is analogous to neutrino oscillations and thus depends on the particle masses [360]. For a large mass difference the transition is suppressed by the momentum mismatch of particles with equal energies. Therefore, the Tokyo limit applies only for $m_a \lesssim 0.03 \text{ eV}$. In a next step one will fill the helioscope with a pressurized gas, giving the photon a dispersive mass to overcome the momentum mismatch.

An alternative method is “Bragg diffraction,” which uses the strong electric field of a crystal lattice which has large Fourier components for the required momentum transfer [363, 364, 365]. The experiment has been performed using Ge detectors which were originally built to search for neutrinoless double-beta decay and for WIMP dark matter; the crystal serves simultaneously as a Primakoff “transition agent” and as an x-ray detector. A first limit of the SOLAX Experiment [366] of $g_{a\gamma} \lesssim 27 \times 10^{-10} \text{ GeV}^{-1}$ is not yet compatible with Eq. (1) and thus not self-consistent. In the future one may reach this limit, but prospects to go much further appear dim [367].

The Primakoff conversion of stellar axions can also proceed in the magnetic fields of Sun spots or in the galactic magnetic field so that one might expect anomalous x- or γ -ray fluxes from the Sun [368], the red supergiant Betelgeuse [369], or SN 1987A [370, 371]. Observations of SN 1987A yield $g_{a\gamma} \lesssim 0.1 \times 10^{-10} \text{ GeV}^{-1}$ for nearly massless pseudoscalars with $m_a \lesssim 10^{-9} \text{ eV}$. A similar limit obtains from the isotropy of the cosmic x-ray background which would be modified by the conversion to axions in the galactic magnetic field [372]. Axion-photon conversion in the magnetic fields of stars, the galaxy, or the early universe were also studied in [360, 373, 374, 375, 376, 377, 378, 379, 380], but no additional limits emerged.

The existence of massless pseudoscalars would cause a photon birefringence effect in pulsar magnetospheres, leading to a differential time delay between photons of opposite helicity and thus to $g_{a\gamma} \lesssim 0.5 \times 10^{-10} \text{ GeV}^{-1}$ [381].

A laser beam in a laboratory magnetic field would also be subject to vacuum birefringence [382], adding to the QED Cotton-Mouton effect. First pilot experiments [353, 383] did not reach the QED level. Two vastly improved current projects are expected to get there [384, 385], but they will stay far away from the “axion line” in Fig. 13. With a laser beam in a strong magnet one can also search for Primakoff axion production and subsequent back-conversion, but a pilot experiment naturally did not have the requisite sensitivity [386]. The exclusion range of current laser experiments is schematically indicated in Fig. 13.

The most important limit on the photon coupling of pseudoscalars derives from the helium-burning lifetime of HB stars in globular clusters, i.e. from Eq. (3),

$$g_{a\gamma} \lesssim 0.6 \times 10^{-10} \text{ GeV}^{-1}. \quad (22)$$

For $m_a \gtrsim 10$ keV this limit quickly degrades as the emission is suppressed when the particle mass exceeds the stellar temperature. For a fixed temperature, the Primakoff energy-loss rate decreases with increasing density so that Eq. (2) implies a less restrictive constraint. Equation (22) was first stated in [4], superseding the slightly less restrictive but often-quoted “red-giant bound” of [18]—see the discussion after Eq. (3). The axion relation Eq. (21) leads to

$$m_a C_\gamma \lesssim 0.3 \text{ eV} \quad \text{and} \quad f_a/C_\gamma \gtrsim 2 \times 10^7 \text{ GeV}. \quad (23)$$

In the DFSZ model and grand unified models, $C_\gamma \approx 0.75$ so that $m_a \lesssim 0.4$ eV and $f_a \gtrsim 1.5 \times 10^7$ GeV (Fig. 14). For models in which $E/N = 2$ and thus C_γ is very small, the bounds are significantly weaker.

On the basis of their two-photon coupling alone, pseudoscalars can reach thermal equilibrium in the early universe. Their subsequent $a \rightarrow 2\gamma$ decays would contribute to the cosmic photon backgrounds [352, 354], excluding a non-trivial m_a - $g_{a\gamma}$ -range (Fig. 13). Some of the pseudoscalars would end up in galaxies and clusters of galaxies. Their decay would produce an optical line feature that was not found [387, 388, 389], leading to the “telescope” limits in Fig. 13. For axions, the telescope limits exclude an approximate mass range 4–14 eV even for a small C_γ .

Axions with a mass in the μeV (10^{-6} eV) range could be the dark matter of the universe (Sec. 6.3). The Primakoff conversion in a microwave cavity placed in a strong magnetic field (“haloscope”) allows one to search for galactic dark-matter axions [355]. Two pilot experiments [390, 391] and first results from a full-scale search [392] already exclude a range of coupling strength shown in Fig. 13. The new generation of full-scale experiments [338, 392, 393, 394] should cover the dotted area in Fig. 13, perhaps leading to the discovery of axion dark matter.

6.2.2 Electrons

Pseudoscalars which couple to electrons are produced by the Compton process $\gamma + e^- \rightarrow e^- + a$ [39, 44, 46, 48, 49, 52] and by the electron bremsstrahlung process $e^- + (A, Z) \rightarrow (A, Z) + e^- + a$ [45, 48, 50, 70, 71, 74, 77]. A standard solar model yields an axion luminosity of [48] $L_a = \alpha_{ae} 6.0 \times 10^{21} L_\odot$ where α_{ae} is the axion electron “fine-structure constant” as defined after Eq. (17). The helioseismological constraint $L_a \lesssim 0.1 L_\odot$ of Sec. 2.3 implies $\alpha_{ae} \lesssim 2 \times 10^{-23}$. White-dwarf cooling gives [4, 69] $\alpha_{ae} \lesssim 1.0 \times 10^{-26}$, while the most restrictive limit is from the delay of helium ignition in low-mass red-giants [52] in the spirit of Eq. (2)

$$\alpha_{ae} \lesssim 0.5 \times 10^{-26} \quad \text{or} \quad g_{ae} \lesssim 2.5 \times 10^{-13}. \quad (24)$$

For $m_a \gtrsim T \approx 10$ keV this limit quickly degrades because the emission from a thermal plasma is suppressed. With Eq. (17) one finds for axions

$$m_a C_e \lesssim 0.003 \text{ eV} \quad \text{and} \quad f_a/C_e \gtrsim 2 \times 10^9 \text{ GeV}. \quad (25)$$

In KSVZ-type models $C_e = 0$ at tree level so that no interesting limit obtains. In the DFSZ model $m_a \cos^2 \beta \lesssim 0.01$ eV and $f_a/\cos^2 \beta \gtrsim 0.7 \times 10^9$ GeV. Since $\cos^2 \beta$ can be very small, there is no generic limit on m_a .

6.2.3 Nucleons

The axion-nucleon coupling strength is primarily constrained by the SN 1987A energy-loss argument [119, 120, 121, 122, 123, 124, 125, 126, 127]. The main problem is to estimate the axion emission rate reliably. In the early papers it was based on a somewhat naive calculation of the bremsstrahlung process $NN \rightarrow NNa$, using quasi-free nucleons that interact perturbatively through a one-pion exchange potential. Assuming an equal axion coupling g_{aN} to protons and neutrons this treatment leads to the g_{aN} -dependent shortening of the SN 1987A neutrino burst of Fig. 8. However, in a dense medium the bremsstrahlung process likely saturates, reducing the naive emission rate by as much as an order of magnitude [126]. With this correction, and assuming that the neutrino burst

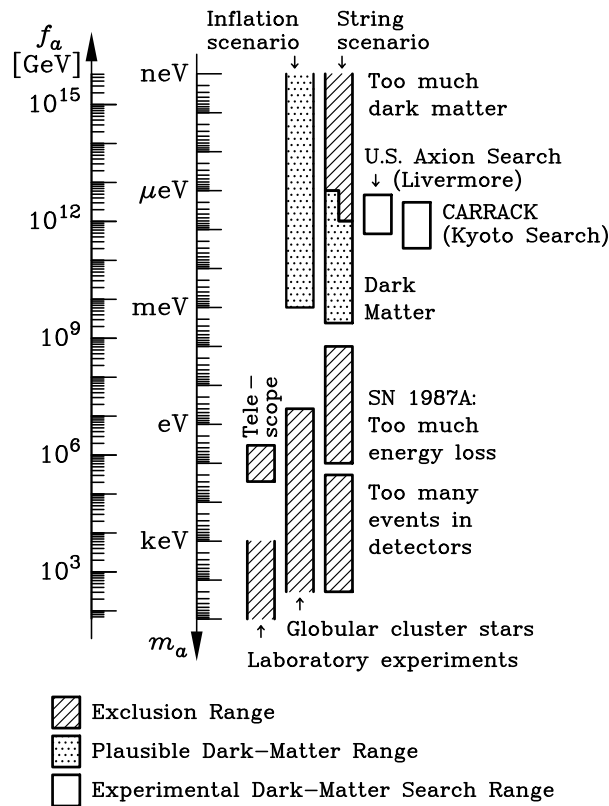


Figure 14: Astrophysical and cosmological exclusion regions (hatched) for the axion mass m_a , or equivalently the Peccei-Quinn scale f_a . The globular-cluster limit depends on the axion-photon coupling; it was assumed that $E/N = 8/3$ as in GUT models or the DFSZ model. The SN 1987A limits depend on the axion-nucleon couplings; the shown case corresponds to the KSVZ model and approximately to the DFSZ model. The dotted “inclusion regions” indicate where axions could plausibly be the cosmic dark matter. Most of the allowed range in the inflation scenario requires fine-tuned initial conditions. In the string scenario the plausible dark-matter range is somewhat controversial as indicated by the step in the low-mass end of the “inclusion bar.” Also shown is the projected sensitivity range of the search experiments for galactic dark-matter axions.

was not shortened by more than half, one reads from Fig. 8 an excluded range

$$3 \times 10^{-10} \lesssim g_{aN} \lesssim 3 \times 10^{-7}. \quad (26)$$

With Eq. (17) this implies an exclusion range

$$0.002 \text{ eV} \lesssim m_a C_N \lesssim 2 \text{ eV} \quad \text{and} \quad 3 \times 10^6 \text{ GeV} \lesssim f_a / C_N \lesssim 3 \times 10^9 \text{ GeV}. \quad (27)$$

For KSVZ axions the coupling to neutrons disappears while $C_p \approx -0.34$. With a proton fraction of about 0.3 one estimates an effective $C_N \approx 0.2$ so that [4, 126]

$$0.01 \text{ eV} \lesssim m_a \lesssim 10 \text{ eV} \quad \text{and} \quad 0.6 \times 10^6 \text{ GeV} \lesssim f_a \lesssim 0.6 \times 10^9 \text{ GeV} \quad (28)$$

is excluded.

In a detailed numerical study the values for C_n and C_p appropriate for the KSVZ model and for the DFSZ model with different choices of $\cos^2 \beta$ were implemented [127]. For KSVZ axions one finds a limit $m_a \lesssim 0.008 \text{ eV}$, while it varies between about 0.004 and 0.012 eV for DFSZ axions, depending on $\cos^2 \beta$. In view of the large overall uncertainties it is probably good enough to remember $m_a \lesssim 0.01 \text{ eV}$ as a generic limit (Fig. 14).

Axions on the “strong interaction side” of the exclusion range Eq. (26) would have produced excess counts in the neutrino detectors by their absorption on oxygen if $1 \times 10^{-6} \lesssim g_{aN} \lesssim 1 \times 10^{-3}$ [169]. For KSVZ axions this crudely translates into $20 \text{ eV} \lesssim m_a \lesssim 20 \text{ keV}$ as an exclusion range (Fig. 14).

6.2.4 Hadronic Axion Window

This limit as well as the “trapping side” of the energy-loss argument have not been studied in as much detail because the relevant m_a range is already excluded by the globular-cluster argument (Fig. 14) which, however, depends on the axion-photon interaction which would nearly vanish in models with $E/N = 2$. In this case a narrow gap of allowed axion masses in the neighborhood of 10 eV may exist between the two SN arguments (“hadronic axion window”).

In this region one can derive interesting limits from globular-cluster stars where axions can be emitted by nuclear processes, causing a metallicity-dependent modification of the core mass at helium ignition [51]. It is intriguing that in this window axions could play a cosmological role as a hot dark matter component [395]. Usually, of course, axions are a *cold* dark matter candidate. Moreover, in this window it may be possible to detect a 14.4 keV monochromatic solar axion line which is produced by transitions between the first excited and ground state of ^{57}Fe . In the laboratory one can then search for axion absorption which would give rise to x-rays as ^{57}Fe de-excites [396]. A recent pilot experiment did not have enough sensitivity to find axions [397], but a vastly improved detector is now in preparation in Tokyo (private communication by S. Moriyama and M. Minowa).

6.3 Cosmological Limits

The astrophysical axion mass limits are particularly interesting when juxtaposed with the cosmological ones which we thus briefly review. For $f_a \gtrsim 10^8 \text{ GeV}$ cosmic axions never reach thermal equilibrium in the early universe. They are produced by a nonthermal mechanism that is intimately intertwined with their Nambu-Goldstone nature and that implies that their contribution to the cosmic

density is proportional to $f_a^{1.175}$ and thus to $m_a^{-1.175}$. The requirement not to “overclose” the universe with axions thus leads to a *lower* mass limit.

One must distinguish between two generic cosmological scenarios. If inflation occurred after the Peccei-Quinn symmetry breaking or if $T_{\text{reheat}} < f_a$, the initial axion field takes on a constant value $a_i = f_a \Theta_i$ throughout the universe, where $0 \leq \Theta_i < \pi$ is the initial “misalignment” of the QCD Θ parameter [398, 399, 400, 401]. If $\Theta_i \sim 1$ one obtains a critical density in axions for $m_a \sim 1 \mu\text{eV}$, but since Θ_i is unknown there is no strict cosmological limit on m_a . However, the possibility to fine-tune Θ_i is limited by inflation-induced quantum fluctuations which in turn lead to temperature fluctuations of the cosmic microwave background [402, 403, 404, 405]. In a broad class of inflationary models one thus finds an upper limit to m_a where axions could be the dark matter. According to the most recent discussion [405] it is about 10^{-3} eV (Fig. 14).

If inflation did not occur at all or if it occurred before the Peccei-Quinn symmetry breaking with $T_{\text{reheat}} > f_a$, cosmic axion strings form by the Kibble mechanism [406, 407]. Their motion is damped primarily by axion emission rather than gravitational waves. After axions acquire a mass at the QCD phase transition they quickly become nonrelativistic and thus form a cold dark matter component. Unknown initial conditions no longer enter, but details of the string mechanism are sufficiently complicated to prevent an exact prediction of the axion density. On the basis of Battye and Shellard’s treatment [408, 409] and assuming that axions are the cold dark matter of the universe one finds a plausible mass range of $m_a = 6\text{--}2500 \mu\text{eV}$ [3]. Sikivie et al. [410, 411, 412] predict somewhat fewer axions, allowing for somewhat smaller masses if axions are the dark matter.

Either way, the ongoing full-scale search experiments for galactic dark matter axions (Sec. 6.2.1 and Fig. 13) in Livermore (U.S. Axion Search [392]) and in Kyoto (CARRACK [393, 394]) aim at a cosmologically well-motivated range of axion masses (Fig. 14).

7 LONG-RANGE FORCES

7.1 Fifth Force

New low-mass scalar or vector bosons would mediate long-range forces between macroscopic bodies. This is in contrast with pseudoscalars which couple to the spin and thus produce no long-range force between unpolarized bodies except for a residual force from two-boson exchange [413, 414, 415]. In stars, a new long-range force has two different consequences. First, it modifies the effect of gravity. Second, it drains the star of energy, for the quanta of the new force are massless, or nearly so, and thus arise in thermal reactions.

Thermal graviton emission is a case in point [416, 417, 418, 419, 420]. However, the graviton luminosity is very small, about $10^{-19} L_\odot$ for the Sun. Naturally, the coherent large-scale force is the most important aspect of gravity in stars! This conclusion carries over to new forces, notably a putative “fifth force.” According to experiment, a fifth force has to be much weaker than gravity [421, 422, 423, 424] so that possible modifications of stellar structure [425, 426] or the solar p-mode frequencies [427, 428] are too small to be observable. Likewise, modifications of fundamental coupling constants near pulsars [429] or scalar boson emission by the Hulse-Taylor binary pulsar [430] are negligible effects.

However, there are no experimental fifth-force limits below about the centime-

ter scale, corresponding to boson masses exceeding about 10^{-3} eV, where the most restrictive bounds arise from the energy loss of stars. The Yukawa coupling g_S (g_V) of scalar (vector) bosons ϕ to electrons has been constrained by the bremsstrahlung process $e^- + {}^4\text{He} \rightarrow {}^4\text{He} + e^- + \phi$ which leads with Eq. (3) to limits of $g_S \lesssim 1.3 \times 10^{-14}$ and $g_V \lesssim 0.9 \times 10^{-14}$ [4, 56, 57]. The Yukawa coupling to baryons has been constrained by the Compton process $\gamma + {}^4\text{He} \rightarrow {}^4\text{He} + \phi$, leading to $g_S \lesssim 4.3 \times 10^{-11}$ and $g_V \lesssim 3.0 \times 10^{-11}$ [4, 56, 57].

7.2 Leptonic and Baryonic Gauge Interactions

It has been speculated that lepton and baryon number could play the role of gauge charges [431, 432]. One consequence would be the existence of long-range leptonic and baryonic forces. The globular-cluster limits of the previous section translate into $e_L \lesssim 1 \times 10^{-14}$ and $e_B \lesssim 3 \times 10^{-11}$ on the leptonic and baryonic gauge charges. Tests of the equivalence principle on solar-system scales constrain a composition-dependent fifth force, leading to something like $e_{L,B} \lesssim 10^{-23}$ [433]. The cosmic background neutrinos would screen leptonic forces over large distances, but the solar-system limit on e_L remains unaffected [113]. On the other hand, the SN 1987A neutrino burst would not suffer dispersion in the leptonic field of the galaxy because it is shielded by the cosmic background neutrinos [113]. Leptonic forces contribute to the neutrino self-energy, modifying matter-induced neutrino oscillations in the Sun and supernovae [434, 435].

7.3 Time-Variation of Newton's Constant

Astrophysics and cosmology are natural laboratories for testing all conceivable deviations from the standard theory of gravitation [436]. One hypothesis, which goes back to Dirac's large numbers hypothesis [437, 438], holds that the value of Newton's constant G_N evolves in time. The present-day rate of change can be measured by a precision study of the orbits of celestial bodies. In the solar system data come from laser ranging of the Moon [439] and radar ranging of the planets, notably by the Viking landers on Mars [440]. The increase of the length of day from 1663–1972 caused by tidal forces in the Earth-Moon system are consistent with a constant G_N [441], although some controversial claims for a decreasing G_N have been raised [436]. Beginning in 1974, very precise orbital data exist for the Hulse-Taylor binary pulsar PSR 1923+16 [442]. A weaker but less model-dependent bound arises from the spin-down rate of the pulsar PSR 0655+64 [443]. Finally, the long-time stability of galaxy clusters limits a decreasing G_N [444]. The bounds from these methods are summarized in Table 2.

Very intriguing limits follow from the properties of the Sun. Paleontological evidence for its past luminosity, which scales approximately as $G_N^7 \mathcal{M}^5$, provides limits on previous values of G_N [445]. Solar models with a time-varying G_N were studied in the 1960s and 1970s [446, 447, 448, 449, 450, 451, 452], but truly interesting limits arose only recently from helioseismological observations [453, 454, 455]. A limit $|\dot{G}_N/G_N| \lesssim 2 \times 10^{-12} \text{ yr}^{-1}$ was derived by a comparison of the measured small-spacing p-mode frequency differences with those calculated from solar models with a time-varying G_N [455]. The authors believe that the uncertainty is dominated by the observational errors while the prime systematic uncertainty is the exact solar age. A more conservative approach was used in deriving limits on a new solar energy loss mechanism (Sec. 2.3). The helioseismo-

Table 2: Range of allowed time variation of Newton’s constant.

Method	\dot{G}_N/G_N [10^{-12} yr $^{-1}$]		Authors	Year	Ref.
	from	to			
Laser ranging (Moon)	−8	8	Williams et al.	1996	[439]
Radar ranging (Mars)	−12	8	Shapiro	1990	[440]
Length of day	−20	20	Morrison	1973	[441]
Binary Pulsar 1913+16	0	22	Damour & Taylor	1991	[442]
Spin-down PSR 0655+64	−55	55	Goldman	1990	[443]
Stability galaxy clusters	−60	—	Dearborn & Schramm	1974	[444]
Helioseismology	−2	2	Guenther et al.	1998	[455]
Globular-cluster ages	−35	7	Degl’Innocenti et al.	1996	[461]
Pulsar masses	−5	4	Thorsett	1996	[462]

logical analysis of [455] provides the most restrictive limit on \dot{G}_N/G_N , hopefully stimulating other groups to re-assess the bound independently.

A large effect is expected on the oldest stars which “integrate” $G_N(t)$ into the distant past. White-dwarf cooling is a case in point [456, 457]. Under reasonable assumptions for the galactic age, the faint end of the luminosity function prefers a negative value for \dot{G}_N/G_N around -10 to -30×10^{-12} yr $^{-1}$ [457]. Very recently this case has been re-examined [458] in greater detail. The observational uncertainty of the faint end of the luminosity function and the uncertainty of the galactic age preclude a clear limit on \dot{G}_N/G_N . However, it is remarkable that even values as small as 10^{-14} yr $^{-1}$ seem to make a noticeable difference for the cooling behavior of the oldest white dwarfs.

Globular clusters are another important case because a different G_N in the past changes their apparent age based on the brightness of the main-sequence turn-off [459, 460, 461]. A comparison with the expansion age of the universe brackets the allowed rate-of-change to the interval shown in Table 2.

A very sensitive limit arises from the observed masses of several old pulsars which measure the value of G_N at their time of formation in a SN explosion [462]. The mass of a SN core at the time of collapse depends on its Chandrasekhar value which in turn scales as $G_N^{-3/2}$.

The limits shown in Table 2 are difficult to compare on an equal footing as they involve vastly different ways of dealing with statistical and systematic uncertainties. However, it looks fair to conclude that $|\dot{G}_N/G_N|$ cannot exceed a few 10^{-12} yr $^{-1}$ and that stars play an important role in this discourse. A similar bound arises from the cosmic expansion rate at the time of big-bang nucleosynthesis as measured by the primordial light-element abundances [463]. It implies that three minutes after the big bang G_N agreed with its present-day value to within a few tens of percent. A comparison of this limit with those of Table 2 requires a specific assumption about the functional dependence of $G_N(t)$.

7.4 Equivalence Principle

The general relativistic equivalence principle implies that the space-time trajectories of relativistic particles are independent of internal degrees of freedom such

as spin or flavor, and independent of the particle type (e.g. photon, neutrino). Several astronomical observations allow tests of this prediction.

Limits on a gravitationally induced birefringence effect for photon propagation have been derived from the absence of depolarization of the Zeeman components of spectral lines emitted in magnetically active regions of the Sun [464]. Observations of the light deflection by the Sun could soon become interesting [465]. The depolarization effect on distant radio galaxies already provides very restrictive limits [466, 467], as do pulsar observations [468, 469, 470].

One may also test for the equality of the Shapiro time delay between different particles which propagate through the same gravitational field. The absence of an anomalous shift between the SN 1987A photon and neutrino arrival times (Sec. 4.2) gave limits on violations of the equivalence principle [116, 117, 118]. The observation of a future galactic SN could provide independent arrival information for $\bar{\nu}_e$ and ν_e and thus provide another such test [108, 471].

A violation of the equivalence principle could manifest itself by a relative shift of the energies of different neutrino flavors in a gravitational field. For a given momentum p the matrix of energies in flavor space (relativistic limit) is $E = p + M^2/2p + 2p\phi(\mathbf{r})(1 + F)$ where M^2 is the squared neutrino mass matrix, $\phi(\mathbf{r})$ the Newtonian gravitational potential, and F a matrix of dimensionless constants which parametrize the violation of the equivalence principle. $F \neq 0$ can lead to neutrino oscillations in analogy to the standard vacuum oscillations which are caused by the matrix M^2 [472, 473, 474, 475, 476, 477, 478, 479, 480, 481, 482, 483, 484]. Values for F_{ij} in the general $10^{-14} - 10^{-17}$ range could account for the solar neutrino problem.

7.5 Photon Mass

While it is usually taken for granted that photons are strictly massless, this theoretical expectation still needs to be tested experimentally. Some of the most restrictive constraints are related to the long-range nature of static electric or magnetic fields. The best laboratory limit of $m_\gamma \lesssim 10^{-14}$ eV derives from a test of Coulomb's law—see [485] for a review.

In the astrophysical domain, the dispersion of the pulsed signal of radio pulsars is not a very sensitive diagnostic as the interstellar medium mimics a photon mass corresponding to a plasma frequency of order 10^{-11} eV. The spatial variation of magnetic fields of celestial bodies is far more sensitive. Jupiter's magnetic field as measured by Pioneer-10 yields $m_\gamma \lesssim 0.6 \times 10^{-15}$ eV [486] while the Earth's field gives $m_\gamma \lesssim 0.8 \times 10^{-15}$ eV [487].

If the photon has a mass, Am_γ^2 is an observable quantity where A is the vector potential corresponding to known magnetic fields. A recent laboratory experiment discloses $Am_\gamma^2 \lesssim 0.8 \times 10^{-22}$ T m eV² [488]. The galactic magnetic field implies $A \approx 2 \times 10^9$ T m (Tesla-meter) so that $m_\gamma \lesssim 2 \times 10^{-16}$ eV while a cluster-level field corresponds to $A \approx 10^{12}$ T m, providing $m_\gamma \lesssim 10^{-17}$ eV.

Even more restrictive limits obtain from astrophysical objects in which magnetic fields, and hence the Maxwellian form of electrodynamics, play a key role at maintaining equilibrium or creating long-lived stable structures [489]. The most restrictive case is based on an argument about the magneto-gravitational equilibrium of the gas in the Small Magellanic Cloud. The argument requires that the range of the interaction exceeds the characteristic field scale of about 3 kpc [490]. This resulting limit $m_\gamma \lesssim 10^{-27}$ eV, if correct, is surprisingly close to

10^{-33} eV where the photon Compton wavelength would exceed the radius of the observable universe and thus would cease to have any observable consequences.

7.6 *Multibody Neutrino Exchange*

Two-neutrino exchange between fermions gives rise to a long-range force. A neutrino may also pass around several fermions, so to speak, producing a much smaller potential. In a thought-provoking paper it was claimed that this multibody neutrino exchange could be a huge effect in neutron stars, essentially because combinatorial factors among many neutrons win out against the smallness of the potential [491]. To stabilize neutron stars, it was claimed, the long-range nature of neutrino exchange had to be suppressed by a nonvanishing mass exceeding about 0.4 eV for all flavors. In an interesting series of papers it was shown, however, that a proper resummation of a seemingly divergent series of terms leads to a well-behaved and small “neutron-star self-energy” [492, 493, 494, 495, 496, 497], invalidating the claim of a lower neutrino mass limit.

8 CONCLUSION

Stellar-evolution theory together with astronomical observations, the SN 1987A neutrino burst, and certain x- and γ -ray observations provide a number of well-developed arguments to constrain the properties of low-mass particles. The most successful examples are globular-cluster stars where the “energy-loss argument” was condensed into the simple criteria of Eqs. (2) and (3) and SN 1987A where it was summarized by Eq. (5). New particle-physics conjectures must first pass these and other simple astrophysical standard tests before being taken too seriously.

A showcase example for the interplay between astrophysical limits with laboratory experiments and cosmological arguments is provided by the axion hypothesis. The laboratory and astrophysical limits push the Peccei-Quinn scale to such high values that it appears almost inevitable that axions, if they exist at all, play an important role as a cold dark matter component. This makes the direct search for galactic axion dark matter a well-motivated effort. Other important standard limits pertain to neutrino electromagnetic form factors—laboratory experiments will have a difficult time catching up.

The globular-cluster limit was based on relatively old observational data. A plot like Fig. 5 could be made more significant with dedicated CCD observations of globular clusters and improved theoretical interpretations. Assuming that such an effort produces internally consistent results, the statistical significance would improve, but I would not expect a vast gain for, say, the neutrino magnetic-moment limit as there always remain irreducible systematic uncertainties.

Shockingly, SN 1987A as a particle-physics laboratory is based on no more than two dozen measured neutrinos. The observation of a future galactic SN with a large detector like Superkamiokande or a future observatory such as OMNIS [247] would provide a high-statistics neutrino light curve and thus a sound empirical basis for SN theory in general and for particle-physics interests in particular. Alas, galactic supernovae happen only once every few decades, perhaps only once per century. Thus, while the neutrinos from the next galactic SN surely are on their way, it could be a long wait until they arrive.

Most of the theoretical background relevant to this field could not be touched

upon in this brief overview. The physics of weakly coupled particles in stars is a nice playing field for “particle physics in media” which involves field theory at finite temperature and density (FTD), many-body effects, particle dispersion and reactions in magnetic fields and media, oscillations of trapped neutrinos, and so forth. It is naturally in the context of SN theory where such issues are of particular interest, but even the plasmon decay $\gamma \rightarrow \nu\bar{\nu}$ in normal stars or the MSW effect in the Sun are interesting cases. Particle physics in media and its astrophysical and cosmological applications is a fascinating topic in its own right which well deserves a dedicated review.

Much more information of particle-physics interest may be written in the sky than has been deciphered as yet. Other objects or phenomena should be considered, perhaps other kinds of conventional stars, perhaps more exotic phenomena such as γ -ray bursts. The particle-physics lessons to be learned from them are left to be reviewed in a future report!

ACKNOWLEDGMENTS

This work was supported, in part, by the Deutsche Forschungsgemeinschaft under grant No. SFB-375.

Literature Cited

1. Turner MS. *Phys. Rept.* 197:67 (1990)
2. Raffelt GG. *Phys. Rept.* 198:1 (1990)
3. Caso C, et al. *Eur. Phys. J. C* 3:1 (1998)
4. Raffelt GG. *Stars as Laboratories for Fundamental Physics*. Chicago: University of Chicago Press (1996)
5. Bahcall J. *Neutrino Astrophysics*. Cambridge: Cambridge University Press (1989).
6. Castellani V, et al. *Phys. Rept.* 281:309 (1997)
7. Bahcall JN, Krastev PI, Smirnov AY. *Phys. Rev. D* 58:096016 (1998)
8. Glendenning NK. *Compact Stars*. New York: Springer (1997)
9. Weber F. *Superdense Hadronic Matter and Relativistic Stars*. Bristol: Institute of Physics (1998)
10. Alcock C, Olinto AV. *Annu. Rev. Nucl. Part. Sci.* 38:161 (1988)
11. Madsen J, Haensel P (editors). *Strange Quark Matter in Physics and Astrophysics, Nucl. Phys. B (Proc. Suppl.)* vol. 24B (1992)
12. Vassiliadis G, et al (editors). *Proc. Int. Symp. Strangeness and Quark Matter, Sept. 1–5, 1994, Crete, Greece*. Singapore: World Scientific (1995)
13. Kolb EW, Turner MS. *The Early Universe*. Reading, Mass.: Addison-Wesley (1990)
14. Freese K, Krasteva E. *Phys. Rev. D* 59:063004 (1999)
15. Jungman G, Kamionkowski M, Griest K. *Phys. Rept.* 267:195 (1996)
16. Frieman JA, Dimopoulos S, Turner MS. *Phys. Rev. D* 36:2201 (1987)
17. Schlattl H, Weiss A, Raffelt G. *Astropart. Phys.*, in press (1999)
18. Raffelt G, Dearborn D. *Phys. Rev. D* 36:2211 (1987)
19. Christensen-Dalsgaard J, Thompson DO, Gough DO. *Astrophys. J.* 378:413 (1991)
20. Degl’Innocenti S, Dziembowski WA, Fiorentini G, Ricci B. *Astropart. Phys.* 7:77 (1997)
21. Basu S, et al. *Mon. Not. R. Astr. Soc.* 292:243, (1997)
22. Carlson ED, Salati P. *Phys. Lett B* 218:79 (1989)
23. Raffelt G, Starkman G. *Phys. Rev. D* 40:942 (1989)
24. Buonanno R, et al. *Mem. Soc. Astron. Ital.* 57:391 (1986)
25. Renzini A, Fusi Pecci F. *Annu. Rev. Astron. Astrophys.* 26:199 (1988)
26. Clayton DD. *Principles of Stellar Evolution and Nucleosynthesis*. Chicago: University of Chicago Press (1968)
27. Kippenhahn R, Weigert A. *Stellar Structure and Evolution*. Berlin: Springer (1990)
28. Raffelt G. *Astrophys. J.* 365:559 (1990)

29. Castellani M, Degl'Innocenti S. *Astrophys. J.* 402:574 (1993)
30. Catelan M, de Freitas Pacheco JA, Horvath JE. *Astrophys. J.* 461:231 (1996)
31. Buzzoni A, et al. *Astron. Astrophys.* 128:94 (1983)
32. Raffelt G, Dearborn D. *Phys. Rev. D* 37:549 (1988)
33. Sutherland P, et al. *Phys. Rev. D* 13:2700 (1976)
34. Fukugita M, Yazaki S. *Phys. Rev. D* 36:3817 (1987)
35. Raffelt G, Dearborn D, Silk J. *Astrophys. J.* 336:64 (1989)
36. Raffelt GG. *Phys. Rev. Lett.* 64:2856 (1990)
37. Raffelt G, Weiss A. *Astron. Astrophys.* 264:536 (1992)
38. Dicus DA, et al. *Phys. Rev. D* 18:1829 (1978)
39. Mikaelian KO. *Phys. Rev. D* 18:3605 (1978)
40. Dicus DA, et al. *Phys. Rev. D* 22:839 (1980)
41. Georgi H, Glashow SL, Nussinov S. *Nucl. Phys. B* 193:297 (1981)
42. Barroso A, Branco GC. *Phys. Lett. B* 116:247 (1982)
43. Fukugita M, Watamura S, Yoshimura M. *Phys. Rev. Lett.* 48:1522 (1982)
44. Fukugita M, Watamura S, Yoshimura M. *Phys. Rev. D* 26:1840 (1982)
45. Krauss LM, Moody JE, Wilczek F. *Phys. Lett. B* 144:391 (1984)
46. Brodsky SJ, et al. *Phys. Rev. Lett.* 56:1763 (1986)
47. Pantziris A, Kang K. *Phys. Rev. D* 33:3509 (1986)
48. Raffelt G. *Phys. Rev. D* 33:897 (1986)
49. Chanda R, Nieves JF, Pal PB. *Phys. Rev. D* 37:2714 (1988)
50. Raffelt G. *Phys. Rev. D* 41:1324 (1990)
51. Haxton WC, Lee KY. *Phys. Rev. Lett.* 66:2557 (1991)
52. Raffelt G, Weiss A. *Phys. Rev. D* 51:1495 (1995)
53. Hoffmann S. *Phys. Lett. B* 193:117 (1987)
54. Raffelt G. *Phys. Rev. D* 38:3811 (1988)
55. van der Velde JC. *Phys. Rev. D* 39:1492 (1989)
56. Grifols JA, Massó E. *Phys. Lett. B* 173:237 (1986)
57. Grifols JA, Massó E, Peris S. *Mod. Phys. Lett. A* 4:311 (1989)
58. Bouquet A, Vayonakis CE. *Phys. Lett. B* 116:219 (1982)
59. Fukugita M, Sakai N. *Phys. Lett. B* 114:23 (1982)
60. Anand JD, et al. *Phys. Rev. D* 29:1270 (1984)
61. Sweigart AV, Gross PG. *Astrophys. J. Suppl.* 36:405 (1978)
62. Shapiro SL, Teukolsky SA. *Black Holes, White Dwarfs, and Neutron Stars*, New York: John Wiley (1983)
63. Fleming TA, Liebert J, Green RF. *Astrophys. J.* 308:176 (1986)
64. Liebert J, Dahn CC, Monet DG. *Astrophys. J.* 332:891 (1988)
65. Koester D, Schönberner D. *Astron. Astrophys.* 154:125 (1986)
66. Mestel L. *Mon. Not. R. Astr. Soc.* 112:583 (1952)
67. Kepler SO, et al. *Astrophys. J.* 378:L45 (1991)
68. Kepler SO, et al. *Baltic Astron.* 4:221 (1995)
69. Raffelt G. *Phys. Lett. B* 166:402 (1986)
70. Nakagawa M, Kohyama Y, Itoh N. *Astrophys. J.* 322:291 (1987)
71. Nakagawa M, et al. *Astrophys. J.* 326:241 (1988)
72. Wang J. *Mod. Phys. Lett. A* 7:1497 (1992)
73. Blinnikov SI, Dunina-Barkovskaya NV. *Mon. Not. R. Astr. Soc.* 266:289 (1994)
74. Altherr T, Petitgirard E, del Río Gaztelurrutia T. *Astropart. Phys.* 2:175 (1994)
75. Isern J, Hernanz M, García-Berro E. *Astrophys. J.* 392:L23 (1992)
76. Tsuruta S. *Phys. Rept.* 292:1 (1998)
77. Iwamoto N. *Phys. Rev. Lett.* 53:1198 (1984)
78. Tsuruta S, Nomoto K. In: *Observational Cosmology*, ed. by A. Hewitt et al, IAU Symposium No. 124 (1987)
79. Umeda H, et al. In: *Proc. Neutron Stars and Pulsars, 17–20 Nov. 1997, Tokyo, Japan*, ed. by N. Shibazaki et al., Singapore: World Scientific (1998)
80. Iwamoto N, et al. *Phys. Rev. D* 51:348 (1995)
81. Umeda H, Nomoto K, Tsuruta S. *Astrophys. J.* 431:309 (1994)
82. Umeda H, Tsuruta S, Nomoto K. *Astrophys. J.* 433:256 (1994)
83. Suy IS, Lee CH. *Phys. Lett. B* 432:145 (1998)
84. Schramm DN, Truran JW. *Phys. Rept.* 189:89 (1990)

85. Raffelt GG. *Mod. Phys. Lett. A* 5:2581 (1990)
86. Koshiha M. *Phys. Rept.* 220:229 (1992)
87. Brown GE, Bethe HA, Baym G. *Nucl. Phys. A* 375:481 (1982)
88. Bethe HA. *Rev. Mod. Phys.* 62:801 (1990)
89. Petschek AG (editor). *Supernovae*. New York: Springer (1990)
90. Cooperstein J. *Phys. Rept.* 163:95 (1988)
91. Burrows A. *Annu. Rev. Nucl. Part. Sci.* 40:181 (1990)
92. Janka HT. In: *Proc. Vulcano Workshop 1992: Frontier Objects in Astrophysics and Particle Physics*, ed. by F. Giovannelli and G. Mannocchi. *Conf. Proc. Soc. Ital. Fis.* Vol. 40 (1993)
93. Hirata KS, et al. *Phys. Rev. D* 38:448 (1988)
94. Bratton CB, et al. *Phys. Rev. D* 37:3361 (1988)
95. Alexeyev EN, et al. *Pis'ma Zh. Eksp. Teor. Fiz.* 45:461 (1987) [*JETP Lett.* 45:589 (1987)]
96. Loredo TJ, Lamb DQ. In: *Proc. Fourteenth Texas Symposium on Relativistic Astrophysics*, ed. by E. J. Fenyves, *Ann. N.Y. Acad. Sci.* 571:601 (1989)
97. Loredo TJ. *From Laplace to Supernova SN 1987A: Bayesian Inference in Astrophysics*. Ph.D. Thesis, University of Chicago (1995)
98. Janka HT, Hillebrandt W. *Astron. Astrophys.* 224:49 (1989)
99. Jegerlehner B, Neubig F, Raffelt G. *Phys. Rev. D* 54:1194 (1996)
100. Lattimer JM, Yahil A. *Astrophys. J.* 340:426 (1989)
101. LoSecco JM. *Phys. Rev. D* 39:1013 (1989)
102. Kielczewska D. *Phys. Rev. D* 41:2967 (1990)
103. Zatspein GI. *Pis'ma Zh. Eksp. Teor. Fiz.* 8:333 (1968) [*JETP Lett.* 8:205 (1968)]
104. Kernan PJ, Krauss LM. *Nucl. Phys. B* 437:243 (1995)
105. Barbiellini G, Cocconi G. *Nature* 329:21 (1987)
106. Fujiwara K. *Phys. Rev. D* 39:1764 (1989)
107. Atzmon E, Nussinov S. *Phys. Lett. B* 328:103 (1994)
108. Pakvasa S, Simmons WA, Weiler TJ. *Phys. Rev. D* 39:1761 (1989)
109. Grifols JA, Massó E, Peris S. *Phys. Lett. B* 207:493 (1988)
110. Grifols JA, Massó E, Peris S. *Astropart. Phys.* 2:161 (1994)
111. Fiorentini G, Mezzorani G. *Phys. Lett. B* 221:353 (1989)
112. Malaney RA, Starkman GD, Tremaine S. *Phys. Rev. D* 51:324 (1995)
113. Dolgov AD, Raffelt GG. *Phys. Rev. D* 52:2581 (1995)
114. Longo MJ. *Phys. Rev. D* 36:3276 (1987)
115. Stodolsky L. *Phys. Lett. B* 201:353 (1988)
116. Krauss LM, Tremaine S. *Phys. Rev. Lett.* 60:176 (1988)
117. Coley AA, Tremaine S. *Phys. Rev. D* 38:2927 (1988)
118. Almeida LD, Matsas GEA, Natale AA. *Phys. Rev. D* 39:677 (1989)
119. Ellis J, Olive KA. *Phys. Lett. B* 193:525 (1987)
120. Raffelt G, Seckel D. *Phys. Rev. Lett.* 60:1793 (1988)
121. Turner MS. *Phys. Rev. Lett.* 60:1797 (1988)
122. Mayle R, et al. *Phys. Lett. B* 203:188 (1988)
123. Mayle R, et al. *Phys. Lett. B* 219:515 (1989)
124. Burrows A, Turner MS, Brinkmann RP. *Phys. Rev. D* 39:1020 (1989)
125. Burrows A, Ressel T, Turner MS. *Phys. Rev. D* 42:3297 (1990)
126. Janka HT, Keil W, Raffelt G, Seckel D. *Phys. Rev. Lett.* 76:2621 (1996)
127. Keil W, et al. *Phys. Rev. D* 56:2419 (1997)
128. Grifols JA, Massó E, Peris S. *Phys. Lett. B* 215:593 (1988)
129. Aharonov Y, Avignone III FT, Nussinov S. *Phys. Rev. D* 37:1360 (1988)
130. Aharonov Y, Avignone III FT, Nussinov S. *Phys. Lett. B* 200:122 (1988)
131. Aharonov Y, Avignone III FT, Nussinov S. *Phys. Rev. D* 39:985 (1989)
132. Choi K, Kim CW, Kim J, Lam WP. *Phys. Rev. D* 37:3225 (1988)
133. Choi K, Santamaria A. *Phys. Rev. D* 42:293 (1990)
134. Chang S, Choi K. *Phys. Rev. D* 49:12 (1994)
135. Ellis J, et al. *Phys. Lett. B* 215:404 (1988)
136. Lau K. *Phys. Rev. D* 47:1087 (1993)
137. Nowakowski M, Rindani SD. *Phys. Lett. B* 348:115 (1995)
138. Grifols JA, Massó E, Peris S. *Phys. Lett. B* 220:591 (1989)
139. Grifols JA, Mohapatra RN, Riotto A. *Phys. Lett. B* 400:124 (1997)
140. Grifols JA, Mohapatra RN, Riotto A. *Phys. Lett. B* 401:283 (1997)

141. Grifols JA, Massó E, Toldra R. *Phys. Rev. D* 57:614 (1998)
142. Dicus DA, Mohapatra RN, Teplitz VL. *Phys. Rev. D* 57:578 (1998); (E) *ibid.* 57:4496 (1998)
143. Arkani-Hamed N, Dimopoulos S, Dvali G. *Phys. Rev. D* 59:086004 (1999)
144. Cullen S, Perelstein M. hep-ph/9903422
145. Gaemers KJF, Gandhi R, Lattimer JM. *Phys. Rev. D* 40:309 (1989)
146. Grifols JA, Massó E. *Phys. Lett. B* 242:77 (1990)
147. Gandhi R, Burrows A. *Phys. Lett. B* 246:149 (1990); (E) *ibid.* 261:519 (1991)
148. Mayle R, et al. *Phys. Lett. B* 317:119 (1993)
149. Maalampi J, Peltoniemi JT. *Phys. Lett. B* 269:357 (1991)
150. Turner MS. *Phys. Rev. D* 45:1066 (1992)
151. Pantaleone J. *Phys. Rev. D* 46:510 (1992)
152. Burrows A, Gandhi R, Turner MS. *Phys. Rev. Lett.* 68:3834 (1992)
153. Goyal A, Dutta S. *Phys. Rev. D* 49:3910 (1994)
154. Babu KS, Mohapatra RN, Rothstein IZ. *Phys. Rev. D* 45:5 (1992)
155. Babu KS, Mohapatra RN, Rothstein IZ. *Phys. Rev. D* 45:3312 (1992)
156. Kainulainen K, Maalampi J, Peltoniemi JT. *Nucl. Phys. B* 358:435 (1991)
157. Raffelt G, Sigl G. *Astropart. Phys.* 1:165 (1993)
158. Barbieri R, Mohapatra RN. *Phys. Rev. D* 39:1229 (1989)
159. Grifols JA, Massó E. *Nucl. Phys. B* 331:244 (1990)
160. Grifols JA, Massó E, Rizzo TG. *Phys. Rev. D* 42:3293 (1990)
161. Rizzo TG. *Phys. Rev. D* 44:202 (1991)
162. Lattimer JM, Cooperstein J. *Phys. Rev. Lett.* 61:23 (1988)
163. Barbieri R, Mohapatra RN. *Phys. Rev. Lett.* 61:27 (1988)
164. Goyal A, Dutta S. *Phys. Rev. D* 49:5593 (1994)
165. Goyal A, Dutta S, Choudhury SR. *Phys. Lett. B* 346:312 (1995)
166. Ayala A, D'Olivo JC, Torres M. hep-ph/9804230
167. Mohapatra RN, Rothstein IZ. *Phys. Lett. B* 247:593 (1990)
168. Grifols JA, Massó E. *Phys. Rev. D* 40:3819 (1989)
169. Engel J, Seckel D, Hayes AC. *Phys. Rev. Lett.* 65:960 (1990)
170. Dodelson S, Frieman JA, Turner MS. *Phys. Rev. Lett.* 68:2572 (1992)
171. Chupp EL, Vestrand WT, Reppin C. *Phys. Rev. Lett.* 62:505 (1989)
172. Oberauer L, et al. *Astropart. Phys.* 1:377 (1993)
173. von Feilitzsch F, Oberauer L. *Phys. Lett. B* 200:580 (1988)
174. Kolb EW, Turner MS. *Phys. Rev. Lett.* 62:509 (1989)
175. Bludman SA. *Phys. Rev. D* 45:4720 (1992)
176. Jaffe AH, Turner MS. *Phys. Rev. D* 55:7951 (1997)
177. Miller RS. *A Search for Radiative Neutrino Decay and its Potential Contribution to the Cosmic Diffuse Gamma-Ray Flux*. Ph.D. Thesis, Univ. New Hampshire (1995)
178. Miller RS, Ryan JM, Svoboda RC. *Astron. Astrophys. Suppl. Ser.* 120:635 (1996)
179. Dar A, Dado S. *Phys. Rev. Lett.* 59:2368 (1987)
180. Mohapatra RN, Nussinov S, Zhang X. *Phys. Rev. D* 49:3434 (1994)
181. Schmid H, Raffelt G, Leike A. *Phys. Rev. D* 58:113004 (1998)
182. Dar A, Goodman J, Nussinov S. *Phys. Rev. Lett.* 58:2146 (1987)
183. Dar A. Report, Institute for Advanced Study, unpublished (1987)
184. Nussinov S, Rephaeli Y. *Phys. Rev. D* 36:2278 (1987)
185. Goldman I, et al. *Phys. Rev. Lett.* 60:1789 (1988)
186. Voloshin MB. *Phys. Lett. B* 209:360 (1988)
187. Okun LB. *Yad. Fiz.* 48:1519 (1988) [*Sov. J. Nucl. Phys.* 48:967 (1988)]
188. Blinnikov SI, Okun LB. *Pis'ma Astron. Zh.* 14:867 (1988) [*Sov. Astron. Lett.* 14:368 (1988)]
189. Falk SW, Schramm DN. *Phys. Lett. B* 79:511 (1978)
190. Takahara M, Sato K. *Phys. Lett. B* 174:373 (1986)
191. Mikheyev SP, Smirnov AY. *Zh. Eksp. Teor. Fiz.* 91:7 (1986) [*Sov. Phys. JETP* 64:4 (1986)]
192. Arafune J, et al. *Phys. Rev. Lett.* 59:1864 (1987)
193. Arafune J, et al. *Phys. Lett. B* 194:477 (1987)
194. Lagage PO, et al. *Phys. Lett. B* 193:127 (1987)
195. Minakata H, et al. *Mod. Phys. Lett. A* 2:827 (1987)
196. Nötzold D. *Phys. Lett. B* 196:315 (1987)
197. Walker TP, Schramm DN. *Phys. Lett. B* 195:331 (1987)
198. Kuo TK, Pantaleone J. *Phys. Rev. D* 37:298 (1988)

199. Minakata H, Nunokawa H. *Phys. Rev. D* 38:3605 (1988)
200. Rosen SP. *Phys. Rev. D* 37:1682 (1988)
201. Fuller GM, et al. *Astrophys. J.* 389:517 (1992)
202. Janka HT, Hillebrandt W. *Astron. Astrophys. Suppl.* 78:375 (1989)
203. Janka HT. *Astropart. Phys.* 3:377 (1995)
204. Hardy S, Janka HT, Raffelt G. *Work in progress.* (1999)
205. Suzuki H. *Num. Astrophys. Japan* 2:267 (1991)
206. Suzuki H. In: *Frontiers of Neutrino Astrophysics, Proc. of the International Symposium on Neutrino Astrophysics, 19–22 Oct. 1992, Takayama/Kamioka, Japan*, ed. by Y. Suzuki and K. Nakamura. Tokyo: Universal Academy Press (1993)
207. Hannestad S, Raffelt G. *Astrophys. J.* 507:339 (1998)
208. Woosley SE, Hoffmann RD. *Astrophys. J.* 395:202 (1992)
209. Meyer BS, et al. *Astrophys. J.* 399:656 (1992)
210. Wittl J, Janka HT, Takahashi K. *Astron. Astrophys.* 286:841 (1994)
211. Takahashi K, Wittl J, Janka HT. *Astron. Astrophys.* 286:857 (1994)
212. Meyer BS. *Annu. Rev. Astron. Astrophys.* 32:153 (1994)
213. Meyer BS. *Astrophys. J.* 449:L55 (1995)
214. Meyer BS, McLaughlin GC, Fuller GM. *Phys. Rev. C* 58:3696 (1998)
215. Qian YZ, et al. *Phys. Rev. Lett.* 71:1965 (1993)
216. Qian YZ, Fuller GM. *Phys. Rev. D* 51:1479 (1995)
217. Sigl G. *Phys. Rev. D* 51:4035 (1995)
218. Pantaleone J. *Phys. Lett. B* 342:250 (1995)
219. Laughlin GC, et al. astro-ph/9902106
220. Kusenko A, Segrè G. *Phys. Rev. Lett.* 77:4872 (1996)
221. Qian YZ. *Phys. Rev. Lett.* 79:2750 (1997)
222. Kusenko A, Segrè G. *Phys. Rev. Lett.* 79:2751 (1997)
223. Kusenko A, Segrè G. *Phys. Lett. B* 396:197 (1997)
224. Akhmedov EK, Lanza A, Sciama DW. *Phys. Rev. D* 56:6117 (1997)
225. Grasso D, Nunokawa H, Valle JWF. *Phys. Rev. Lett.* 81:2412 (1998)
226. Horvat R. *Mod. Phys. Lett. A* 13:2379 (1998)
227. Kusenko A, Segrè G. *Phys. Rev. D* 59:061302 (1999)
228. Janka HT, Raffelt GG. *Phys. Rev. D* 59:023005 (1999)
229. Smirnov AY, Spergel DN, Bahcall JN. *Phys. Rev. D* 49:1389 (1994)
230. Valle JWF. In: *Proc. New Trends in Neutrino Physics, Tegernsee, Ringberg Castle, Germany, 24–29 May 1998*, to be published; hep-ph/9809234
231. Kayser B. In: *Proc. 29th International Conference on High-Energy Physics (ICHEP 98), Vancouver, Canada, 23–29 July 1998*, to be published; hep-ph/9810513
232. Smirnov A. *Proc. 5th International WEIN Symposium: A Conference on Physics Beyond the Standard Model (WEIN 98), Santa Fe, New Mexico, 14–21 June 1998*, to be published; hep-ph/9901208
233. Fukuda Y, et al (Superkamiokande Collaboration). *Phys. Rev. Lett.* 81:1562 (1998)
234. Athanassopoulos C, et al. *Phys. Rev. Lett.* 77:3082 (1996)
235. Athanassopoulos C, et al. *Phys. Rev. Lett.* 81:1774 (1998)
236. Nunokawa H, Peltoniemi JT, Rossi A, Valle JWF. *Phys. Rev. D* 56:1704 (1997)
237. Qian YZ, Fuller GM. *Phys. Rev. D* 49:1762 (1994)
238. Choubey S, Majumdar D, Kar K. hep-ph/9809424
239. Fuller GM, Haxton WC, McLaughlin GC. astro-ph/9809164
240. Totani T. *Phys. Rev. Lett.* 80:2039 (1998)
241. Seckel D, Steigman G, Walker T. *Nucl. Phys. B* 366:233 (1991)
242. Krauss LM, et al. *Nucl. Phys. B* 380:507 (1992)
243. Fiorentini G, Acerbi C. *Astropart. Phys.* 7:245 (1997)
244. Beacom JF, Vogel P. *Phys. Rev. D* 58:093012 (1998)
245. Beacom JF, Vogel P. *Phys. Rev. D* 58:053010 (1998)
246. Cline D, et al. *Phys. Rev. D* 50:720 (1994)
247. Smith PF. *Astropart. Phys.* 8:27 (1997)
248. Morrison DRO. *Nature* 366:29 (1993)
249. Mohapatra RN, Pal P. *Massive Neutrinos in Physics and Astrophysics*. Singapore: World Scientific (1991)
250. Winter K (editor). *Neutrino Physics*. Cambridge: Cambridge University Press (1991)

251. Lucio JL, Rosado A, Zepeda A. *Phys. Rev. D* 31:1091 (1985)
252. Auriemma G, Srivastava Y, Widom A. *Phys. Lett. B* 195:254 (1987)
253. Degrassi G, Sirlin A, Marciano WJ. *Phys. Rev. D* 39:287 (1989)
254. Musolf MJ, Holstein BR. *Phys. Rev. D* 43:2956 (1991)
255. Góngora A, Stuart RG. *Z. Phys. C* 55:101 (1992)
256. Salati P. *Astropart. Phys.* 2:269 (1994)
257. D’Olivo JC, Nieves JF, Pal PB. *Phys. Rev. D* 40:3679 (1989)
258. Altherr T, Salati P. *Nucl. Phys. B* 421:662 (1994)
259. Adams JB, Ruderman MA, Woo CH. *Phys. Rev.* 129:1383 (1963)
260. Zaidi MH. *Nuovo Cim.* 40:502 (1965)
261. Haft M, Raffelt G, Weiss A. *Astrophys. J.* 425:222 (1994); (E) *ibid.* 438:1017 (1995)
262. Bernstein J, Ruderman MA, Feinberg G. *Phys. Rev.* 132:1227 (1963)
263. Brogini C, et al (MUNU Collaboration). *Nucl. Phys. B (Proc.Suppl)* 70:188 (1999)
264. Oberauer L, von Feilitzsch F, Mössbauer RL. *Phys. Lett. B* 198:113 (1987)
265. Cowsik R. *Phys. Rev. Lett.* 39:784 (1977)
266. Raffelt G. *Phys. Rev. D* 31:3002 (1985)
267. Ressel MT, Turner MS. *Comments Astrophys.* 14:323 (1990)
268. Biller SD, et al. *Phys. Rev. Lett.* 80:2992 (1998)
269. Raffelt, GG. *Phys. Rev. Lett.* 81:4020 (1998)
270. Henry RC, Feldmann PD. *Phys. Rev. Lett.* 47:618 (1981)
271. Davidsen AF, et al. *Nature* 351:128 (1991)
272. Ioannissyan A, Raffelt G. *Phys. Rev. D* 55:7038 (1997)
273. Elmfors P, Enqvist K, Raffelt G, Sigl G. *Nucl. Phys. B* 503:3 (1997)
274. Fujikawa K, Shrock R. *Phys. Rev. Lett.* 45:963 (1980)
275. Okun LB. *Yad. Fiz.* 44:847 (1986) [*Sov. J. Nucl. Phys.* 44:546 (1986)]
276. Wertz CW. Unpublished (1970), quoted after [277]
277. Cisneros A. *Astrophys. Space Sci.* 10:87 (1971)
278. Voloshin MB, Vysotskiĭ MI. *Yad. Fiz.* 44:845 (1986) [*Sov. J. Nucl. Phys.* 44:544 (1986)]
279. Nötzold D. *Phys. Rev. D* 38:1658 (1988)
280. Schechter J, Valle JWF. *Phys. Rev. D* 24:1883 (1981); (E) *ibid.* 25:283 (1982)
281. Voloshin MB, Vysotskiĭ MI, Okun LB. *Yad. Fiz.* 44:677 (1986) [*Sov. J. Nucl. Phys.* 44:440 (1986)]
282. Voloshin MB, Vysotskiĭ MI, Okun LB. *Zh. Eksp. Teor. Fiz.* 91:754 (1986); (E) *ibid.* 92:368 (1987) [*Sov. Phys. JETP* 64:446; (E) *ibid.* 65:209 (1987)]
283. Akhmedov EK. *Yad. Fiz.* 48:599 (1988) [*Sov. J. Nucl. Phys.* 48:382 (1988)]
284. Akhmedov EK. *Phys. Lett. B* 213:64 (1988)
285. Barbieri R, Fiorentini G. *Nucl. Phys. B* 304:909 (1988)
286. Lim CS, Marciano WJ. *Phys. Rev. D* 37:1368 (1988)
287. Akhmedov EK, Lanza A, Petcov ST. *Phys. Lett. B* 348:124 (1995)
288. Guzzo MM, Nunokawa H. hep-ph/9810408
289. Barbieri R, et al. *Phys. Lett. B* 259:119 (1991)
290. Fiorentini G, Moretti M, Villante FL. *Phys. Lett. B* 413:378 (1997)
291. Pastor S, Semikoz VB, Valle JWF. *Phys. Lett. B* 423:118 (1998)
292. Athar H, Peltoniemi JT, Smirnov AY. *Phys. Rev. D* 51:6647 (1995)
293. Totani T, Sato K. *Phys. Rev. D* 54:5975 (1996)
294. Akhmedov EK, Lanza A, Petcov ST, Sciama DW. *Phys. Rev. D* 55:515 (1997)
295. Brügggen M. *Phys. Rev. D* 55:5876 (1997)
296. Nunokawa H, Qian YZ, Fuller GM. *Phys. Rev. D* 55:3265 (1997)
297. Babu KS, Mohapatra RN. *Phys. Rev. D* 42:3866 (1990)
298. Maruno M, Takasugi E, Tanaka M. *Prog. Theor. Phys.* 86:907 (1991)
299. Takasugi E, Tanaka M. *Prog. Theor. Phys.* 87:679 (1992)
300. Babu KS, Mohapatra RN, Rothstein IZ. *Phys. Rev. D* 45:R3312 (1992)
301. Foot R, Lew H, Volkas RR. *J. Phys. G: Nucl. Part. Phys.* 19:361 (1993); (E) *ibid.* 19:1067 (1993)
302. Holdom B. *Phys. Lett. B* 166:196 (1986)
303. Dobroliubov MI, Ignatiev AY. *Phys. Rev. Lett.* 65:679 (1990)
304. Davidson S, Campbell B, Bailey D. *Phys. Rev. D* 43:2314 (1991)
305. Babu KS, Volkas RR. *Phys. Rev. D* 46:R2764 (1992)
306. Mohapatra RN, Nussinov S. *Int. J. Mod. Phys. A* 7:3817 (1992)

307. Davidson S, Peskin M. *Phys. Rev. D* 49:2114 (1994)
308. Baumann J, et al. *Phys. Rev. D* 37:3107 (1988)
309. Marinelli M, Morpurgo G. *Phys. Lett. B* 137:439 (1984)
310. Prinz AA, et al. *Phys. Rev. Lett.* 81:1175 (1998)
311. Jodidio A, et al. *Phys. Rev. D* 34:1967 (1986); (E) *ibid.* 37:237 (1988)
312. Ellis J, Enqvist K, Nanopoulos DV, Sarkar S. *Phys. Lett. B* 167:457 (1986)
313. Gelmini GB, Roncadelli M. *Phys. Lett. B* 99:411 (1981)
314. Chicashige Y, Mohapatra RN, Peccei RD. *Phys. Lett. B* 98:265 (1981)
315. Berezhiani ZG, Smirnov AY, Valle JWF. *Phys. Lett. B* 291:99 (1992)
316. Kikuchi H, Ma E. *Phys. Lett. B* 335:444 (1994)
317. Kolb EW, Turner MS. *Phys. Rev. D* 36:2895 (1987)
318. Kolb EW, Tubbs DL, Dicus DA. *Astrophys. J.* 255:L57 (1982)
319. Dicus DA, Kolb EW, Tubbs DL. *Nucl. Phys. B* 223:532 (1983)
320. Manohar A. *Phys. Lett. B* 192:217 (1987)
321. Konoplich RV, Khlopov MY. *Yad. Fiz.* 47:891 (1988) [*Sov. J. Nucl. Phys.* 47:565 (1988)]
322. Fuller GM, Mayle R, Wilson JR. *Astrophys. J.* 332:826 (1988)
323. Berezhiani ZG, Smirnov AY. *Phys. Lett. B* 220:279 (1989)
324. Valle JWF. *Phys. Lett. B* 199:432 (1987)
325. Langacker P, London D. *Phys. Rev. D* 38:907 (1988)
326. Guzzo MM, Masiero A, Petcov ST. *Phys. Lett. B* 260:154 (1991)
327. Roulet E. *Phys. Rev. D* 44:935 (1991)
328. Barger V, Phillips RJN, Whisnant K. *Phys. Rev. D* 44:1629 (1991)
329. Bergmann S. *Nucl. Phys. B* 515:363 (1998)
330. Nunokawa H, Qian YZ, Rossi A, Valle JWF. *Phys. Rev. D* 54:4356 (1996)
331. Bergmann S, Kagan A. *Nucl. Phys. B* 538:368 (1999)
332. Peccei RD, Quinn HR. *Phys. Rev. Lett.* 38:1440 (1977)
333. Peccei RD, Quinn HR. *Phys. Rev. D* 16:1791 (1977)
334. Weinberg S. *Phys. Rev. Lett.* 40:223 (1978)
335. Wilczek F. *Phys. Rev. Lett.* 40:279 (1978)
336. Kim JE. *Phys. Rept.* 150:1 (1987)
337. Cheng HY. *Phys. Rept.* 158:1 (1988)
338. Sikivie P. *Proc. Axion Workshop, Univ. of Florida, Gainesville, Florida, USA, 13-15 March 1998*, to be published in *Nucl. Phys. B (Proc. Suppl.)* (1999)
339. Carena M, Peccei RD. *Phys. Rev. D* 40:652 (1989)
340. Choi K, Kang K, Kim JE. *Phys. Rev. Lett.* 62:849 (1989)
341. Turner MS, Kang HS, Steigman G. *Phys. Rev. D* 40:299 (1989)
342. Iwamoto N. *Phys. Rev. D* 39:2120 (1989)
343. Dine M, Fischler W, Srednicki M. *Phys. Lett. B* 104:199 (1981)
344. Zhitnitskiĭ AP. *Yad. Fiz.* 31:497 (1980) [*Sov. J. Nucl. Phys.* 31:260 (1980)]
345. Kim JE. *Phys. Rev. Lett.* 43:103 (1979)
346. Shifman MA, Vainshtein AI, Zakharov VI. *Nucl. Phys. B* 166:493 (1980)
347. Kaplan DB. *Nucl. Phys. B* 260:215 (1985)
348. Cheng SL, Geng CQ, Ni WT. *Phys. Rev. D* 52:3132 (1995)
349. Kim JE. *Phys. Rev. D* 58:055006 (1998)
350. Raffelt G. *Phys. Rev. D* 37:1356 (1988)
351. Massó E, Toldrà R. *Phys. Rev. D* 52:1755 (1995)
352. Massó E, Toldrà R. *Phys. Rev. D* 55:7967 (1997)
353. Cameron R, et al. *Phys. Rev. D* 47:3707 (1993)
354. Mori F. *Mod. Phys. Lett. A* 11:715 (1996)
355. Sikivie P. *Phys. Rev. Lett.* 51:1415 (1983); (E) *ibid.* 52:695 (1984)
356. van Bibber K, Morris D, McIntyre P, Raffelt G. *Phys. Rev. D* 39:2089 (1989)
357. Lazarus DM, et al. *Phys. Rev. Lett.* 69:2333 (1992)
358. Moriyama S, et al. *Phys. Lett. B* 434:147 (1998)
359. Moriyama S. *Direct Search for Solar Axions by Using Strong Magnetic Field and X-Ray Detectors*. Ph.D. Thesis (in English), University of Tokyo (1998)
360. Raffelt G, Stodolsky L. *Phys. Rev. D* 37:1237 (1988)
361. Vorob'ev PV, Kolokolov IV. astro-ph/9501042
362. Zioutas K, et al. astro-ph/9801176, submitted to *Nucl. Instrum. Methods. A*
363. Buchmüller W, Hoogeveen F. *Phys. Lett. B* 237:278 (1990)

364. Paschos EA, Zioutas K. *Phys. Lett. B* 323:367 (1994)
365. Creswick RJ, et al. *Phys. Lett. B* 427:235 (1998)
366. SOLAX Collaboration (Avignone III FT, et al). *Phys. Rev. Lett.* 81:5068 (1998)
367. Cebrián S, et al. *Astropart. Phys.*, in press (1999)
368. Carlson ED, Tseng LS. *Phys. Lett. B* 365:193 (1996)
369. Carlson ED. *Phys. Lett. B* 344:245 (1995)
370. Brockway JW, Carlson ED, Raffelt GG. *Phys. Lett. B* 383:439 (1996)
371. Gifols JA, Massó E, Toldrà R. *Phys. Rev. Lett.* 77:2372 (1996)
372. Krasnikov SV. *Phys. Rev. Lett.* 76:2633 (1996)
373. Morris DE. *Phys. Rev. D* 34:843 (1986)
374. Yoshimura M. *Phys. Rev. D* 37:2039 (1988)
375. Yanagida T, Yoshimura M. *Phys. Lett. B* 202:301 (1988)
376. Gnedin YN, Krasnikov SV. *Zh. Eksp. Teor. Fiz.* 102:1729 (1992) [*Sov. Phys. JETP* 75:933 (1992)]
377. Gnedin YN, Krasnikov SV. *Astron. Lett.* 20:72 (1994)
378. Gnedin YN. *Comments Astrophys.* 18:257 (1996)
379. Gnedin YN. *Astrophys. Space Sci.* 249:125 (1997)
380. Carlson ED, Garretson WD. *Phys. Lett. B* 336:431 (1994)
381. Mohanty S, Nayak SN. *Phys. Rev. Lett.* 70:4038 (1993); (E) *ibid.* 71:1117 (1993); (E) *ibid.* 76:2825 (1996)
382. Maiani L, Petronzio R, Zavattini E. *Phys. Lett. B* 175:359 (1986)
383. Semertzidis Y, et al. *Phys. Rev. Lett.* 64:2988 (1990)
384. Bakalov D, et al. *Quantum Semiclass. Opt.* 10:239 (1998)
385. Lee S, et al. *Fermilab Proposal E-877* (1995)
386. Ruoso G, et al. *Z. Phys. C* 56:505 (1992)
387. Bershadly MA, Ressel MT, Turner MS. *Phys. Rev. Lett.* 66:1398 (1991)
388. Ressel MT. *Phys. Rev. D* 44:3001 (1991)
389. Overduin JM, Wesson PS. *Astrophys. J.* 414:449 (1993)
390. Wuensch WU, et al. *Phys. Rev. D* 40:3153 (1989)
391. Hagmann C, et al. *Phys. Rev. D* 42:1297 (1990)
392. Hagmann C, et al. *Phys. Rev. Lett.* 80:2043 (1998)
393. Ogawa I, Matsuki S, Yamamoto K. *Phys. Rev. D* 53:R1740 (1996)
394. Yamamoto K, Matsuki S. In: *Proc. 2nd International Workshop on the Identification of Dark Matter (IDM 98), Buxton, England, 7–11 Sept. 1998*, to be published; hep-ph/9811487
395. Moroi T, Murayama H. *Phys. Lett. B* 440:69 (1998)
396. Moriyama S. *Phys. Rev. Lett.* 75:3222 (1995)
397. Krčmar M, et al. *Phys. Lett. B* 442:38 (1998)
398. Preskill J, Wise M, Wilczek F. *Phys. Lett. B* 120:127 (1983)
399. Abbott L, Sikivie P. *Phys. Lett. B* 120:133 (1983)
400. Dine M, Fischler W. *Phys. Lett. B* 120:137 (1983)
401. Turner MS. *Phys. Rev. D* 33:889 (1986)
402. Lyth DH. *Phys. Lett. B* 236:408 (1990)
403. Turner MS, Wilczek F. *Phys. Rev. Lett.* 66:5 (1991)
404. Linde A. *Phys. Lett. B* 259:38 (1991)
405. Shellard EPS, Battye RA. astro-ph/9802216.
406. Davis RL. *Phys. Lett. B* 180:225 (1986)
407. Davis RL, Shellard EPS. *Nucl. Phys. B* 324:167 (1989)
408. Battye RA, Shellard EPS. *Nucl. Phys. B* 423:260 (1994)
409. Battye RA, Shellard EPS. *Phys. Rev. Lett.* 73:2954 (1994); (E) *ibid.* 76:2203 (1996)
410. Harari D, Sikivie P. *Phys. Lett. B* 195:361 (1987)
411. Hagmann C, Sikivie P. *Nucl. Phys. B* 363:247 (1991)
412. Chang S, Hagmann C, Sikivie P. *Phys. Rev. D* 59:023505 (1999)
413. Grifols JA, Tortosa S. *Phys. Lett. B* 328:98 (1994)
414. Ferrer F, Grifols JA. *Phys. Rev. D* 58:096006 (1998)
415. Ferrer F, Nowakowski M. hep-ph/9810550
416. Papini G, Valluri SR. *Phys. Rept.* 33:51 (1977)
417. Papini G, Valluri SR. *Astron. Astrophys.* 208:345 (1989)
418. Schäfer G, Dehnen H. *Phys. Rev. D* 27:2864 (1983)

419. Gould RJ. *Astrophys. J.* 288:789 (1985)
420. del Campo S, Ford LH. *Phys. Rev. D* 38:3657 (1988)
421. Fischbach E, Talmadge C. *Nature* 356:207 (1992)
422. Fischbach E, Talmadge C. In: *Proc. 31st Rencontres de Moriond: Dark Matter and Cosmology, Quantum Measurements and Experimental Gravitation, Les Arcs, France, 20–27 Jan. 1996.*
423. Fischbach E, Talmadge C. *The Search for Non-Newtonian Gravity.* New York: Springer (1998)
424. Franklin A. *The Rise and Fall of the Fifth Force.* New York: American Institute of Physics (1993)
425. Glass EN, Szamosi G. *Phys. Rev. D* 35:1205 (1987)
426. Glass EN, Szamosi G. *Phys. Rev. D* 39:1054 (1989)
427. Gilliland RL, Däppen W. *Astrophys. J.* 313:429 (1987)
428. Kuhn JR. In: *Advances in Helio- and Asteroseismology,* ed. by J. Christensen-Dalsgaard and S. Frandsen. Dordrecht: Reidel (1988)
429. Ellis J, et al. *Phys. Lett. B* 228:264 (1989)
430. Mohanty S, Panda PK. *Phys. Rev. D* 53:5723 (1996)
431. Lee TD, Yang CN. *Phys. Rev.* 98:1501 (1955)
432. Okun LB. *Yad. Fiz.* 10:358 (1969) [*Sov. J. Nucl. Phys.* 10:206 (1969)]
433. Blinnikov SI, Dolgov AD, Okun LB, Voloshin MB. *Nucl. Phys. B* 458:52 (1996)
434. Horvat R. *Phys. Rev. D* 52:7098 (1995)
435. Horvat R. *Phys. Lett. B* 366:241 (1996)
436. Will CM. *Theory and Experiment in Gravitational Physics—Revised Edition.* Cambridge: Cambridge University Press (1993)
437. Dirac PAM. *Nature* 139:323 (1937)
438. Dirac PAM. *Proc. R. Soc. London A* 165:199 (1938)
439. Williams JG, Newhall XX, Dickey JO. *Phys. Rev. D* 53:6730 (1996)
440. Shapiro II. In: *General Relativity and Gravitation,* ed. by N. Ashby, D. F. Bartlett, W. Wyss. Cambridge: Cambridge University Press (1990)
441. Morrison LV. *Nature* 241:519 (1973)
442. Damour T, Taylor JH. *Astrophys. J.* 366:501 (1991)
443. Goldman I. *Mon. Not. R. Astr. Soc.* 244:184 (1990)
444. Dearborn DS, Schramm DN. *Nature* 247:441 (1974)
445. Teller E. *Phys. Rev.* 73:801 (1948)
446. Gamow G. *Proc. Natl. Acad. Sci.* 57:187 (1967)
447. Pochoda P, Schwarzschild M. *Astrophys. J.* 139:587 (1964)
448. Ezer D, Cameron AGW. *Can. J. Phys.* 44:593 (1966)
449. Roeder RC, Demarque PR. *Astrophys. J.* 144:1016 (1966)
450. Shaviv G, Bahcall JN. *Astrophys. J.* 155:135 (1969)
451. Chin CW, Stothers R. *Nature* 254:206 (1975)
452. Chin CW, Stothers R. *Phys. Rev. Lett.* 36:833 (1976)
453. Demarque P, et al. *Astrophys. J.* 437:870 (1994)
454. Guenther DB, et al. *Astrophys. J.* 445:148 (1995)
455. Guenther DB, Krauss LM, Demarque P. *Astrophys. J.* 498:871 (1998)
456. Vila SC. *Astrophys. J.* 206:213 (1976)
457. García-Berro E, Hernanz M, Isern J, Mochkovitch R. *Mon. Not. R. Astr. Soc.* 277:801 (1995)
458. Benvenuto OG, Althaus LG, Torres DF. *Mon. Not. R. Astron. Soc.,* in press (1999)
459. Prather MJ. *The Effect of a Brans-Dicke Cosmology upon Stellar Evolution and the Evolution of Galaxies.* Ph.D. Thesis, Yale University (1976)
460. VandenBerg DA. *Mon. Not. R. Astr. Soc.* 181:695 (1977)
461. Degl’Innocenti S, et al. *Astron. Astrophys.* 312:345 (1996)
462. Thorsett SE. *Phys. Rev. Lett.* 77:1432 (1996)
463. Malaney RA, Mathews GJ. *Phys. Rept.* 229:145 (1993)
464. Gabriel MD, Haugan MP, Mann RB, Palmer JH. *Phys. Rev. Lett.* 67:2123 (1991)
465. Gabriel MD, Haugan MP, Mann RB, Palmer JH. *Phys. Rev. D* 43:308 (1991)
466. Carroll SM, Field GB. *Phys. Rev. D* 43:3789 (1991)
467. Haugan MP, Kauffmann TF. *Phys. Rev. D* 52:3168 (1995)
468. LoSecco JM, et al. *Phys. Lett. A* 138:5 (1989)

469. Klein JR, Thorsett SE. *Phys. Lett. A* 145:79 (1990)
470. Krisher TP. *Phys. Rev. D* 44:R2211 (1991)
471. LoSecco JM. *Phys. Rev. D* 38:3313 (1988)
472. Gasperini M. *Phys. Rev. D* 38:2635 (1988)
473. Gasperini M. *Phys. Rev. D* 39:3606 (1989)
474. Halprin A, Leung CN. *Phys. Rev. Lett.* 67:1833 (1991)
475. Pantaleone J, Halprin A, Leung CN. *Phys. Rev. D* 47:R4199 (1993)
476. Iida K, Minakata H, Yasuda O. *Mod. Phys. Lett. A* 8:1037 (1993)
477. Minakata H, Nunokawa H. *Phys. Rev. D* 51:6625 (1995)
478. Bahcall JN, Krastev PI, Leung CN. *Phys. Rev. D* 52:1770 (1995)
479. Halprin A, Leung CN, Pantaleone J. *Phys. Rev. D* 53:5365 (1996)
480. Mureika JR. *Phys. Rev. D* 56:2408 (1997)
481. Glashow SL, et al. *Phys. Rev. D* 56:2433 (1997)
482. Halprin A, Leung CN. *Phys. Lett. B* 416:361 (1998)
483. Mansour SW, Kuo TK. hep-ph/9810510
484. Casini H, D'Olivo JC, Montemayor R, Urrutia LF. hep-ph/9811215
485. Goldhaber AS, Nieto MM. *Rev. Mod. Phys.* 43:277 (1971)
486. Davis Jr L, Goldhaber AS, Nieto MM. *Phys. Rev. Lett.* 35:1402 (1975)
487. Fischbach E, et al. *Phys. Rev. Lett.* 73:514 (1994)
488. Lakes R. *Phys. Rev. Lett.* 80:1826 (1998)
489. Barrow JD, Burman RR. *Nature* 307:14 (1984)
490. Chibisov GV. *Sov. Phys. Usp.* 19:624 (1976)
491. Fischbach E. *Annals Phys.* 247:213 (1996)
492. Kiers K, Tytgat MHG. *Phys. Rev. D* 57:5970 (1998)
493. Abada A, Gavela MB, Pène O. *Phys. Lett. B* 387:315 (1996)
494. Abada A, Pène O, Rodríguez-Quintero J. *Phys. Rev. D* 58:073001 (1998)
495. Abada A, Pène O, Rodríguez-Quintero J. hep-ph/9810449
496. Abada A, Pène O, Rodríguez-Quintero J. *Phys. Lett. B* 423:355 (1998)
497. Arafune J, Mimura Y. *Prog. Theor. Phys.* 100:1083 (1998)